A THEORETICAL STUDY OF THE STRUCTURE, ENERGY, AND SHAPE OF NOVEL BORON-NITROGEN HELICES

CSABA E. SZAKACS

A theoretical study of the structure, energy, and shape of novel boron-nitrogen helices

by

© Csaba E. Szakacs

A thesis submitted to the

School of Graduate Studies

in partial fulfillment of the

requirements for the degree of

Doctor of Philosophy

Department of Chemistry

Memorial University

June 2009

St. John's Newfoundland

Abstract

Ab initio self-consistent field molecular orbital and density functional theory calculations have been performed on a series of helical structures comprised of boron-nitrogen analogues of extended hydrogenated helicenes, with helically arranged N fused benzene rings, N fused methylenylnaphthalene fragments, and alternating N benzene units fused to N-1 cyclobutadiene rings as reference structures.

The electronic structure of boron-nitrogen analogues of angular [N]helicenes (N = 5, 6, 7, 12) and [N]phenylenes (N = 5, 6, 7, 13) were investigated at the HF/6-31G(d), B3LYP/6-31G(d), and MP2/6-31G(d)//HF/6-31G(d) levels of theory. It was observed that the presence of an even number N of rings in the boron-nitrogen [N]helicenes leads to the possibility of angular isomers. Their energetics and relative stability was discussed.

Furthermore, the electronic structure and relative stability of three isomeric non-hydrogenated boron-nitrogen helices were investigated at the HF/6-31G(d), B3LYP/6-31G(d), and MP2/6-31G(d)//HF/6-31G(d) levels of theory. According to this study, some of the initially assumed regular helical structures are unstable; two types of the isomeric structures convert to characteristically different equilibrium geometries.

In addition, laterally extended boron-nitrogen analogues of [N]polymethylenylnaphthalenes (N = 6, 8, and 12) were also investigated at the HF/6-31G(d,p) and B3LYP/6-31G(d,p) levels of theory. By alternating the positions of the boron and nitrogen atoms, two very similar structures are possible, the $N_xB_yH_z$ type helix and the

$B_xN_yH_z$ ($y = x - 1$) type helix, which are comprised of an odd number of fused rings. The inclusion of one more ring results in an even number of fused rings, which leads to helical isomerism in these extended boron-nitrogen helices. Their geometries and energetics are also discussed.

Electron density contours were calculated in order to interpret the existing bonding patterns. These structures may provide supramolecular building blocks and macromolecular "springs" with potential use in nanotechnology.

Acknowledgements

First of all, I would like to express my sincere gratitude to my supervisor Prof. Paul G. Mezey for his continuous guidance and valuable advice throughout my research work, and for financial support.

I would like to thank my supervisory committee members, Dr. Raymond A. Poirier and Dr. Erika Merschrod, for their useful suggestions during all these years, and also for proofreading the thesis.

Many thanks go to Dr. Peter L. Warburton, who helped me survive my first days in St. John's, and also for all the discussions we had regarding my research. Much appreciated was also the guidance and help received from Dr. Jenna L. Wang, a former member of our group.

My appreciation goes also to other present or former members of the theoretical group in the Chemistry Department, Eva Simon, Joshua Hollett, Mansour Almatarneh, Mohammad S. Islam, and Aisha El Sherbiny.

Further acknowledgements are due to the Chemistry Department and the School of Graduate Studies at Memorial University of Newfoundland and NSERC for financial support during my PhD program.

I am most grateful to my dear wife, Alina, for her patience, encouragement and unconditional support, and to our beautiful daughter, Dalma, for her gorgeous smiles.

Finally, I would like to extend my special thanks to my parents who have always supported me in any important decision I made in the last 10 years.

Contents

List of Tables

List of Figures

List of Abbreviations and Symbols

Å	Ångström, 10^{-10}m
$\hat{F}$	Fock operator
$\hat{H}$	Hamiltonian operator
∇^2	Laplacian operator
Ψ	Wavefunction
α	Gaussian exponent
χ	Spin orbital
ϵ	Orbital energy
ϕ	Basis function
ν	Frequency
ρ	Electron density
ψ	Spatial orbital
c	Expansion coefficient
E	Energy

f	Force constant
h	Planck constant
S	Overlap matrix
P	Density matrix
a.u.	Atomic units
B3LYP	Becke3-Lee-Yang-Parr
B88	Becke's corrected exchange functional
BN HCNT	Boron-nitride helical conical nanotube
BNNT	Boron-nitride nanotube
DFT	Density Functional Theory
GTF	Gaussian type functions
GTO	Gaussian type orbitals
HF	Hartree-Fock
HK	Hohenberg-Kohn
KS	Kohn-Sham
LCAO	Linear combination of atomic orbitals
LDA	Local density approximation
LYP	Lee-Yang-Parr correlation functional
MO	Molecular orbital
MIDCO	Molecular isodensity contour
MP2	Second-order Møller-Plesset perturbation

SCF	Self consistent field
STO	Slater type orbital
ZPVE	Zero-point vibrational energy
VWN3	Vosko-Wilk-Nusair local correlation functional
XC	Exchange correlation

Chapter 1

Introduction

The foundations of today's modern theoretical computational chemistry were laid down with the appearence of the first postulates in quantum mechanics at the beginning of the last century. Quantum chemistry derived itself from quantum mechanics and it has become an efficient tool to better describe the behavior of the electrons in atoms and atoms in molecules. Although sound theoretical models were constructed, early on, their application was delayed by the lack of computational power.

In the last 40 years however, with the rapid development of computers, theoretical computational chemistry has grown into a powerful branch of chemistry. Today, scientists are using powerful individual computers or numerous computer clusters combined with computational software based on the early as well as new theories and models to attempt to solve, model, and describe chemical problems, structures and reactions. Molecular modelling has benefited from this evolution of theory and appli-

cations. One advantage of modelling is the ability to create virtual representations of new structures and predict the existence of novel, viable molecules. The driving forces of this new kind of virtual research is the already existing chemical knowledge, intuition and curiosity.

Based on these three motivating factors, in the present thesis an attempt is made to theoretically describe some members of a family of novel boron-nitrogen compounds having helical conformations, motivated by the intriguing features of analogous extended helicenes of carbon chemistry. Such spring-like molecules, interesting on their own right, may provide potential flexible building blocks for nanosystems with adjustable features.

The modern era of boron-nitrogen chemistry is considered to date back to the early 1920s,[1] when borazine, one of the early boron-nitrogen analogues of the carbon based benzene, was synthesized.[2] It became obvious that the boron-nitrogen atom pair, being isoelectronic with the carbon-carbon atom pair, could be a likely replacement for the latter in a variety of carbon-based compounds. An early example is that of the boron-nitrogen analogue of naphthalene, first observed experimentally as a product formed during the gas-phase pyrolysis of borazine[3] and which has been characterized experimentally.[4–6]

The successful synthesis of fullerene[7] and carbon based nanotubes[8] acted as a catalyst for further theoretical research,[9–11] eventually leading to the synthesis of

boron-nitride nanotubes[12] (BNNTs) and of the first boron-nitrogen fullerene-like structures.[13, 14] These boron-nitrogen nanostructures have also been shown to have high chemical and thermal stability,[15] making them good candidates as precursors for the synthesis of boron-nitride ceramic materials.[6, 16] Recently, it was shown that some boron-nitrogen compounds might also have hydrogen storage capabilities.[17–20]

Overall, the study of boron-nitrogen clusters and cages,[9, 21–36] boron-nitrogen nanotubes,[37 44] and boron-nitrogen chains[45, 46] attracted considerable interest in the past decade. The majority of these boron-nitrogen nanocompounds can be reconstructed by fusing smaller building blocks such as borazine rings, boron-nitrogen acenes, or boron-nitrogen cyclacenes.

Borazine

The chemistry of borazine and its derivatives is well described,[1] and as benzene's isoelectronic pair, it received considerable attention among theoreticians.[47 55] Studies tackled borazine's aromaticity,[56] the probability of the existence of borazine dimer,[57] and also borazine's ability to form complexes with metals.[58, 59]

Boron-nitrogen acenes

Boron-nitrogen acenes (Figure 1.1) are comprised of a number of linearly fused borazine rings. Whitehead et al.[60] performed Hückel type calculations on molecules containing three fused borazine rings predicting the possibility for the existence of boron-nitrogen polymers containing a larger number of rings. Kar et al.[61] investigated the structure of boron-nitrogen naphthalene and some of its carbon containing

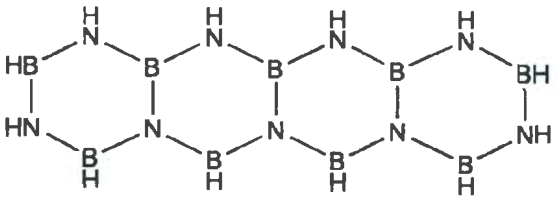

Figure 1.1: Boron-nitrogen acene comprised of four fused rings

derivatives at HF and MP2 levels of theory with the 6-31G(d) and 6-31G+(d) basis sets. Their study revealed that in case of the fully substituted boron-nitrogen naphthalene, while the calculated bond lengths at the HF level were in good agreement with the experimental values, the MP2 values overestimated the experimental bond lengths.

A more recent investigation on these boron-nitrogen compounds involves a theoretical study[62] on the structure and vibronic interactions in boron-nitrogen naphthalene and boron-nitrogen anthracene using density functional theory with the B3LYP/6-31G(d) basis set. Further research involved investigations on the structure and aromaticity of linearly more extended boron-nitrogen acenes (formed by up to five fused borazines, i.e., the boron-nitrogen pentacene) at the density functional B3LYP/6-31+G(d)[63] and B3LYP/6-311+G(d)[64] levels of theory.

Boron-nitrogen cyclacenes

By connecting the ends of the boron-nitrogen acenes, cyclic structures can be formed (Figure 1.2). These are the cyclic boron-nitrogen cyclacenes, the analogues of

the more familiar carbon based cyclacenes.

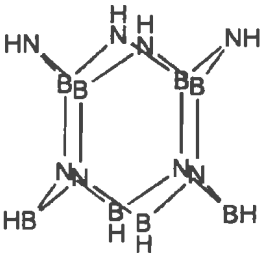

Figure 1.2: Boron-nitrogen cyclacene comprised of four fused rings

Erkoç[65] examined the structure and electronic properties of borazine-based cyclacenes, comprised of up to six fused borazine rings at semiempirical AM1 level of theory. Boron-nitrogen cyclacenes containing a larger number of fused borazine rings were also studied at MNDO and AM1 semiempirical levels of theory.[66] The geometries and energies of these kind of boron-nitrogen cyclacenes were also investigated at the density functional UB3LYP/6-31G(d) level of theory.[67, 68]

Most recently,[69] a comprehensive theoretical study was performed at RHF/6-31G(d) and B3LYP/6-31G(d) levels of theory on boron-nitrogen cyclacenes containing three and four borazine rings, finding that different conformational isomers are possible depending on the direction of the peripheral N-H groups.

From an experimental point of view, the boron-nitrogen nanostructures are being synthesized using a variety of procedures, like arc discharge methods,[12, 70] different

vapor deposition and condensed-phase pyrolysis methods,[16] or polymerization methods.[6]

Scaling back from nanosize to the molecular level, the study of boron-nitrogen cyclacenes and boron-nitrogen acenes containing more than three fused borazine rings remains only at the theoretical level, since, to our knowledge no experimental data is available.

Helicenes can be considered as angular isomers of the acenes. These systems are formed by N fused benzene rings (Figure 1.3), and the phenylenes are structures comprised of N fused benzene rings with N-1 interposed cyclobutadiene rings(Figure 1.4). These carbon based helical structures were extensively studied theoretically.[71–75]

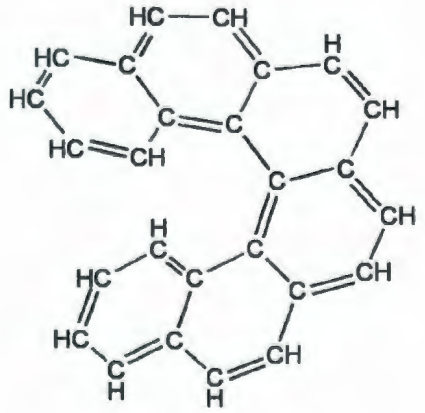

Figure 1.3: Structure of [6]helicene

Helicenic compounds where the carbon atoms in the helix were replaced by other atoms such as nitrogen or sulphur were studied theoretically or experimentally as well.[76–80]

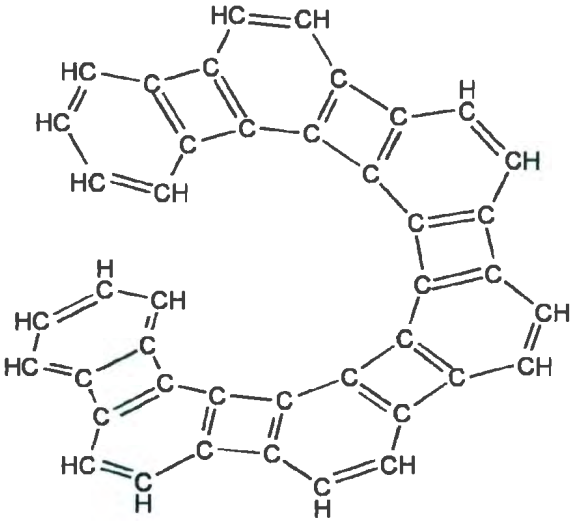

Figure 1.4: Structure of [7]phenylene

However, to our knowledge, detailed theoretical studies of boron-nitrogen analogues of these helical systems have not been reported yet by other research groups.

The boron-nitrogen analogues of helicenes, phenylenes, and some more extended boron-nitrogen analogues of polymethylenylnaphthalenes are the main focus of this thesis, as such molecules possessing helical conformation may become building blocks for more extended novel helical boron-nitride compounds with applications in nan-

otechnology. They could also serve as flexible interconnecting building units in the synthesis of new boron-nitrogen based nanostructures. Since these molecules show analogous shapes with macroscopic springs, it is reasonable to expect that their vibrational properties also show analogies with vibrations, as well as compressibility of macroscopic springs. The aim of this thesis is the theoretical description of the structure, energy, and shape of these boron-nitrogen angular helices and a better understanding of the energetical stability of some of the existing helical isomers. This was achieved through electronic structure calculations using *ab initio* and density functional methods.

It has to be mentioned that this study was also made possible due to the existing computational power available which has experienced a considerable increase in recent years.

The thesis is written in manuscript format and is divided into six chapters, each chapter having its own bibliography except the last chapter which contains conclusions. Chapter 1 begins with an introduction of the overall thesis; Chapter 2 describes the theory behind the methods used throughout the research; Chapter 3, Chapter 4, and Chapter 5 are arranged in manuscript format. Each is subdivided into the following sections: introduction, computational methodology, results and discussion, and summary.

Chapter 3 presents a theoretical study of hydrogenated boron-nitrogen analogues

of helicenes and phenylenes. The presence of an even number N of rings in the boron-nitrogen [N]helicenes leads to the possibility of angular isomers. Their electronic structure and relative stability is discussed.

Having the nonhydrogenated version of helicenes as a starting point, Chapter 4 describes a detailed study of nonhydrogenated fused boron-nitrogen hexagons and decagons. The electronic structure and relative stability of three possible angular isomers are presented.

Chapter 5 introduces some laterally extended boron-nitrogen helical sheets, based on the boron-nitrogen analogue of [N]polymethylenylnaphthalene. By alternating the positions of the boron and nitrogen atoms, two very similar structures containing odd number of fused hexagonal units are possible, the $N_xB_yH_z$ type helix, and the $B_xN_yH_z$ type helix. An even number of fused rings leads to helical isomerism. The geometries and energetics of these helices are investigated.

Some concluding remarks and future directions are presented in Chapter 6.

Bibliography

[1] K. Niedenzu and J. W. Dawson. *Boron-Nitrogen Compounds.* Academic Press Inc., Publishers, New York, 1965.

[2] A. Stock and E. Pohland. *Ber. Dtsch. Chem. Ges.*, 59:2215, 1926.

[3] A. W. Laubengayer, P. C. Moews Jr., and R. F. Porter. *J. Am. Chem. Soc.*, 83:1337, 1961.

[4] G. Mamantov and J. L. Margrave. *J. Inorg. Nucl. Chem.*, 20:348, 1961.

[5] M. A. Neiss and R. F. Porter. *J. Am. Chem. Soc.*, 94:1438, 1972.

[6] P. J. Fazen, E. E. Remsen, J.S. Beck, P.J. Carroll, A. R. McGhie, and L. G. Sneddon. *Chem. Mater.*, 7:1942, 1995.

[7] H. W. Kroto, J. R. Heath, S.C. O'Brien, R. F. Curl, and R. E. Smalley. *Nature*, 318:162, 1985.

[8] S Iijima. *Nature*, 354:56, 1991.

[9] I. Silaghi-Dumitrescu, I. Haiduc, and D. B Sowerby. *Inorg. Chem.*, 32(17):3755, 1993.

[10] X. Xia, D. A. Jelski, J. R. Bowser, and T. F. George. *J. Am. Chem. Soc.*, 114 (16):6493, 1992.

[11] A. Rubio, J. L. Corkill, and M. L. Cohen. *Phys. Rev. B*, 49:5081, 1994.

[12] N. G. Chopra, Luyken R. J., Cherrey K., V. H. Crespi, M. L. Cohen, Louie S. G., and A. Zettl. *Science*, 269:966, 1995.

[13] O. Stephan, Y. Bando, A. Loiseau, F. Willaime, N. Shramchenko, T. Tamiya, and T. Sato. *Appl. Phys. A*, 67:107, 1998.

[14] D. Golberg, Y. Bando, O. Stephan, and K. Kurashima. *Appl. Phys. Lett.*, 73:2441, 1998.

[15] W. Q. Han, W. Mickelson, J. Cumings, and A. Zettl. *Appl. Phys. Lett.*, 81:1110, 2002.

[16] R. T. Paine and C. K. Narula. *Chem. Rev.*, 90:73, 1990.

[17] N. Koi and T. Oku. *Solid State Commun.*, 131:121, 2004.

[18] M. H. Matus, K. D. Anderson, D. M. Camaioni, S. T. Autrey, and D. A. Dixon. *J. Phys. Chem. A*, 111:4411, 2007.

[19] C. R. Miranda and G. Ceder. *J. Chem. Phys.*, 126:184703, 2007.

[20] C. W. Hamilton, R. T. Baker, A. Staubitz, and I. Manners. *Chem. Soc. Rev.*, 38:279, 2009.

[21] G. Seifert, P.W. Fowler, D. Mitchell, D.and Porezag, and Th. Frauenheim. *Chem. Phys. Lett.*, 268:352, 1997.

[22] V. V. Pokropivny, V. V. Skorokhod, G. S. Oleinik, A. V. Kurdyumov, T. S. Bartnitskaya, A. V. Pokropivny, A. G. Sisonyuk, and D.M. Sheichenko. *J. Solid State Chem.*, 154:214, 2000.

[23] T. Oku, A. Nishiwaki, I. Narita, and M. Gonda. *Chem. Phys. Lett.*, 380:620, 2003.

[24] T. Oku, I. Narita, and A. Nishiwaki. *Mater. Manuf. Processes*, 19:1215, 2004.

[25] T. Oku, A. Nishiwaki, and I. Narita. *Sci. Tech. Adv. Mater.*, 5:635, 2004.

[26] T. Oku, A. Nishiwaki, and I. Narita. *Phys. B*, 351:184, 2004.

[27] R. R. Zope, T. Baruah, M. R. Pederson, and B. I. Dunlap. *Chem. Phys. Lett.*, 393:300, 2004.

[28] Y. C. Zhu, Y. Bando, L. W. Yin, and D. Golberg. *Chem. Eur. J.*, 10:3667, 2004.

[29] X. Y. Cui and H. S. Wu. *Chin. J. Chem.*, 23:117, 2005.

[30] H. S. Wu, X. Y. Cui, and X. H. Xu. *J. Mol. Struc.(THEOCHEM)*, 717:107, 2005.

[31] H. S. Wu, X. Y. Cui, F. Qin, X, and H. Jiao. *J. Mol. Struc.(THEOCHEM)*, 714:153, 2005.

[32] S. Xu, M. Zhang, Y. Zhao, B. Chen, J. Zhang, and C. Sun. *Chem. Phys. Lett.*, 418:297, 2006.

[33] R. J. C. Batista, M. S. C. Mazzoni, and H. Chacham. *Chem. Phys. Lett.*, 421:246, 2006.

[34] H. Wang, H. S. Wu, and J. F. Jia. *Chin. J. Chem.*, 24:731, 2006.

[35] W. H. Moon, M. S. Son, and H. J. Hwang. *Appl. Surf. Sci.*, 253:7078, 2007.

[36] S. A. Shevlin, Z. X. Guo, H. J. J. van Dam, P. Sherwood, C. R. A. Catlow, A. A. Sokol, and S. M. Woodley. *Phys. Chem. Chem. Phys.*, 10:1944, 2008.

[37] J.-Ch. Charlier, X. Blase, A. De Vita, and R. Car. *Appl. Phys. A*, 68:267, 1999.

[38] Y. H. Kim, K. J. Chang, and S. G. Louie. *Phys. Rev. B*, 63:205408, 2001.

[39] Z. Peralta-Inga, P. Lane, J. S. Murray, S. Boyd, M. E. Grice, C. J. O'Connor, and P. Politzer. *Nano Letters*, 3:21, 2003.

[40] B. Akdim, R. Pachter, X. Duan, and W. W. Adams. *Phys. Rev. B*, 67:245404, 2003.

[41] H. S. Wu, Xi. H. Xu, F. Q. Zhang, and H. Jiao. *J. Phys. Chem. A*, 107:6609, 2003.

[42] A. S. Barnard, I. K. Snook, and S. P. Russo. *J. Mater. Chem.*, 17:2892, 2007.

[43] B. Baumeier, P. Krger, and J. Pollmann. *Phys. Rev. B*, 76:085407, 2007.

[44] B. J. Cox and J. M. Hill. *J. Phys. Chem. C*, 112:16248, 2008.

[45] J. Zhang, Q. S. Li, and S. Zhang. *Diamond. Relat. Mater.*, 14:1654, 2005.

[46] J. Zhang, Q. S. Li, and S. Zhang. *J. Mol. Struct.(THEOCHEM)*, 715:133, 2005.

[47] R. Hoffmann. *J. Chem. Phys.*, 40(9):2474, 1964.

[48] R. Hoffmann. *Adv. Chem. Ser.*, 42:78, 1964.

[49] O. Chalvet, R. Daudel, and J.J. Kaufman. *Adv. Chem. Ser.*, 42:251, 1964.

[50] O. Chalvet, R. Daudel, and J.J. Kaufman. *J. Am. Chem. Soc.*, 87(3):399, 1965.

[51] J. K. Parker and S. R. Davis. *J. Phys. Chem. A*, 101:9410, 1997.

[52] R. Miao, G. Yang, C. Zhao, J. Hong, and L. Zhu. *J. Mol. Struc.(THEOCHEM)*, 728:197, 2005.

[53] W. Shen, M. Li, Y. Li, and S. Wang. *Inorg. Chim. Acta*, 360:619, 2007.

[54] W. R. Nutt and M. L. McKee. *Inorg. Chem.*, 46:7633, 2007.

[55] B. Anand, H. Nth, H. Schwenk-Kircher, and A. Troll. *Eur. J. Inorg. Chem.*, 20:3186, 2008.

[56] R. Islas, E. Chamorro, J. Robles, T. Heine, J. C. Santos, and G. Merino. *Struct. Chem.*, 18:833, 2007.

[57] S. Kawahara, S. Tsuzuki, and T. Uchimaru. *J. Chem. Phys.*, 119:10081, 2003.

[58] H. S. Kang. *J. Phys. Chem. A*, 109:1458, 2005.

[59] H. Braunschweig, H. Green, K. Radacki, and K. Uttinger. *Dalton Trans.*, 27:3531, 2008.

[60] N.C. Baird and M.A. Whitehead. *Can. J. Chem./Rev. Can. Chim.*, 45(18):2059, 1967.

[61] T. Kar, D. E. Elmore, and S. Scheiner. *J. Mol. Struct.(THEOCHEM)*, 392:65, 1997.

[62] T. Kato and T. Yamabe. *J. Chem. Phys.*, 118:3804, 2003.

[63] A. K. Phukan, R. P. Kalagi, S. R. Gadre, and E. D. Jemmis. *Inorg. Chem.*, 43:5824, 2004.

[64] P. K. Chattaraj and D. R. Roy. *J. Phys. Chem. A*, 111:4684, 2007.

[65] Ş. Erkoç. *J. Mol. Struct.(THEOCHEM)*, 540:153, 2001.

[66] L. Turker. *J. Mol. Struct.(THEOCHEM)*, 640:63, 2003.

[67] K. P. Loh, S. W. Yang, J. M. Soon, H. Zhang, and P. Wu. *J. Phys. Chem. A*, 107:5555, 2003.

[68] S. W. Yang, H. Zhang, J. M. Soon, C. W. Lim, P. Wu, and K. P. Loh. *Diam. Relat. Mater.*, 12:1194, 2003.

[69] C. J. Johnson and R. W. Zoellner. *J. Mol. Struct.(THEOCHEM)*, 893:9, 2009.

[70] A. Loiseau, F. Willaime, N. Demoncy, G. Hug, and H. Pascard. *Phys. Rev. Lett.*, 76:4737, 1996.

[71] J. M. Schulman and R. L. Disch. *J. Am. Chem. Soc.*, 118:8470, 1996.

[72] J. M. Schulman and R. L. Disch. *J. Phys. Chem. A*, 101:5596, 1997.

[73] J. M. Schulman and R. L. Disch. *J. Phys. Chem. A*, 103:6669, 1999.

[74] J. M. Schulman and R. L. Disch. *J. Phys. Chem. A*, 107:5223, 2003.

[75] L. Wang, P. L. Warburton, Z. Szekeres, P. Surjan, and P. G. Mezey. *J. Chem. Inf. Model.*, 45:850, 2005.

[76] K. E. S. Phillips, T. J. Katz, S. Jockusch, A. J. Lovinger, and N. J. Turro. *J. Am. Chem. Soc.*, 123:11899, 2001.

[77] L. Wang and P. G. Mezey. *J. Phys. Chem. A*, 109:3241, 2005.

[78] Y. H. Tian, G Park, and M. Kertesz. *Chem. Mater.*, 20:3266, 2008.

[79] C. Bazzini, T. Caronna, F. Fontana, A. Macchi, P. Mele, I. N. Sora, W. Panzeri, and A. Sironi. *New J. Chem.*, 32:1710, 2008.

[80] C. Li, J. Shi, L. Xu, Y. Wang, Y. Cheng, and H. Wang. *J. Org. Chem.*, 74:408, 2009.

Chapter 2

Theoretical Background

2.1 Hartree-Fock Theory

2.1.1 The Schrödinger Equation

For a detailed description of the microscopic world of atomic or molecular systems and their properties, one must resort to quantum mechanics. By applying the laws of quantum mechanics to chemical problems, one enters into the world of quantum chemistry. Its principles are well outlined in the literature.[1, 2] Accordingly, one of the main goals of the quantum theory of atoms and molecules is solving the Schrödinger equation,

$$\hat{H}\Psi = E\Psi \tag{2.1}$$

where $\hat{H}$ is the Hamiltonian operator, E represents the numerical value of the system's energy (the Hamiltonian operator returns the system energy E as an eigenvalue, as the equation is an eigenvalue equation), and Ψ is a stationary eigenfunction, which depends on the spatial and spin coordinates of all particles making up the system.

The time independent Hamiltonian for n electrons and M nuclei can be written (in atomic units) as the sum of kinetic energy operators and potential energy parts,

$$\hat{H} = -\sum_{i}^{n} \frac{1}{2}\nabla_i^2 - \sum_{A=1}^{M} \frac{1}{2M_A}\nabla_A^2 - \sum_{i=1}^{n}\sum_{A=1}^{M} \frac{Z_A}{r_{iA}} + \sum_{i=1}^{n-1}\sum_{i<j}^{n} \frac{1}{r_{ij}} + \sum_{A=1}^{M-1}\sum_{A<B}^{M} \frac{Z_A Z_B}{R_{AB}} \qquad (2.2)$$

where i and j run over electrons, A and B run over nuclei, M_A is the mass of nucleus A, Z is the atomic number, r_{ij} is the distance between two electrons ($r_{ij} = |\mathbf{r}_i - \mathbf{r}_j|$), r_{iA} is the distance between an electron and a nucleus ($r_{iA} = |\mathbf{r}_{iA}| = |\mathbf{r}_i - \mathbf{R}_A|$), and R_{AB} is the distance between two nuclei ($R_{AB} = |\mathbf{R}_A - \mathbf{R}_B|$). The first term in the equation represents the kinetic energy operator of the electrons; the second term is the operator for the kinetic energy of the nuclei; the third term describes the attraction force between the electrons and the nuclei; the fourth term represents the repulsion between electrons, and the last term the repulsion between the nuclei. The Laplacian operator ∇^2 has the form

$$\nabla^2 = \frac{\partial^2}{\partial x^2} + \frac{\partial^2}{\partial y^2} + \frac{\partial^2}{\partial z^2} \qquad (2.3)$$

Note that the Hamiltonian above is nonrelativistic, and additional terms are needed to fully describe the energy of a system in which the average speed of electrons is approaching the speed of light.

The solution to the stationary Schrödinger equation is the eigenfunction Ψ. For any many-electron system there is a set of Ψ_i solutions with eigenvalues E_i, that is, Eq.(2.1) can have many acceptable solutions, corresponding to different stationary states. The main focus is to find the state with the lowest energy, the ground state.

2.1.2 The Born-Oppenheimer Approximation

The masses of nuclei are much greater than those of the surrounding electrons, and therefore, the nuclei move much more slowly. In one approximation, it can be considered that electrons are changing their positions around the fixed nuclei. Accordingly, it is convenient to suppose that the electron distribution depends only on the positions of the nuclei.

This model is known[3] as the Born - Oppenheimer approximation, and according to it, the Schrödinger equation in the field of fixed nuclei can be written as follows:

$$\hat{H}_{el}\Psi_{el} = E_{el}\Psi_{el} \tag{2.4}$$

where $\hat{H}_{el}$, the electronic Hamiltonian, has the form

$$\hat{H}_{el} = -\sum_{i}^{n} \frac{1}{2}\nabla_i^2 - \sum_{i=1}^{n}\sum_{A=1}^{M} \frac{Z_A}{r_{iA}} + \sum_{i=1}^{n-1}\sum_{i<j}^{n} \frac{1}{r_{ij}} \tag{2.5}$$

The three terms correspond to the kinetic energy, the electron-nuclear attraction, and the electron-electron repulsion. Here Ψ_{el} is the electronic wavefunction, and E_{el} is the electronic energy. Both of them depend directly on the electronic coordinates and parametrically on the nuclear coordinates. The nuclear-repulsion energy V_{NN} is given by

$$\hat{V}_{NN} = \sum_{A=1}^{M-1}\sum_{A<B}^{M} \frac{Z_A Z_B}{R_{AB}} \tag{2.6}$$

Solving Eq.(2.4) and computing V_{NN} from Eq.(2.6) one can get E_{el} for each particular nuclear configuration. Then the energy E_{tot} can be calculated using

$$E_{tot} = E_{el} + V_{NN} \tag{2.7}$$

In this way E_{tot} can be regarded as the net potential function of the nuclear coordinates. Hence it can also be represented as a potential energy curve in case of diatomic molecules and a potential energy surface (hypersurface) in case of polyatomic systems.

2.1.3 Molecular Orbital Theory

Reviewing the electronic Hamiltonian in Eq.(2.5), it can be seen that it is directly related to the coordinates of the electrons. An electron can be described by using one-electron functions or orbitals.[3] The spatial orbital, $\psi(x,y,z)$ is a function of the cartesian coordinates x, y, z, of a single electron, and describes the spatial distribution of an electron. The absolute value of the square of the spatial distribution, $|\psi^2|$ will give the probability density distribution of the electron in space. To describe the electron more accurately, its spin has to be included as well. So, the complete one-electron wavefunction can be represented as the product of a spatial orbital and a spin function, which gives the spin-orbital $\chi(x,y,z,s)$, having the form

$$\chi(x,y,z,s) = \psi(x,y,z)\alpha(s) \tag{2.8}$$

or

$$\chi(x,y,z,s) = \psi(x,y,z)\beta(s) \tag{2.9}$$

depending on the two possible directions of the electron spin, $\alpha(s)$ as spin up($\uparrow$) and $\beta(s)$ as spin down($\downarrow$). However, for n-electron systems one more condition must be fullfilled, that of antisymmetry, which requires that if the spatial and spin coordinates of any two electrons are interchanged, the wavefunction changes sign:

$$\Psi(\chi_1(1), \chi_2(2)..., \chi_i(i), \chi_j(j), ...\chi_n(n)) = -\Psi(\chi_1(1), \chi_2(2)..., \chi_j(j), \chi_i(i), ...\chi_n(n)) \tag{2.10}$$

The simplest way to ensure the above antisymmetry is to arrange the orbitals in a determinantal wavefunction.

$$\Psi = \begin{vmatrix} \chi_1(1) & \chi_2(1) & ... & \chi_n(1) \\ \chi_1(2) & \chi_2(2) & ... & \chi_n(2) \\ . & . & & . \\ . & . & & . \\ . & . & & . \\ \chi_1(n) & \chi_2(n) & ... & \chi_n(n) \end{vmatrix} \tag{2.11}$$

The entire wavefunction has to be normalized, so that the probability of finding the electron in the full space must be 1. If the individual one-electron functions are normalized, and the determinant in Eq.(2.11) is multiplied by a factor of $\frac{1}{\sqrt{(n!)}}$ one gets the Slater determinant[4] for a molecule with even n number of electrons

$$\Psi = \frac{1}{\sqrt{(n!)}} \begin{vmatrix} \chi_1(1) & \chi_2(1) & \cdots & \chi_n(1) \\ \chi_1(2) & \chi_2(2) & \cdots & \chi_n(2) \\ . & . & & . \\ . & . & & . \\ . & . & & . \\ \chi_1(n) & \chi_2(n) & \cdots & \chi_n(n) \end{vmatrix} \tag{2.12}$$

2.1.4 Basis Set Expansion

In practice, the individual molecular orbitals are expressed as linear combinations of a finite set of N one-electron functions or orbitals known as basis functions.[3] Then, the individual orbital ψ_i will have the form,

$$\psi_i = \sum_{\mu=1}^{N} c_{\mu i}\phi_\mu \tag{2.13}$$

where ϕ_μ are elements of a finite basis set, centered at various atoms, and $c_{\mu i}$ are the molecular orbital expansion coefficients.

The most commonly used type of basis functions are the Gaussian type functions or orbitals (GTF's or GTO's), which have the exponential form exp(-α r_{iA}^2) as part

of their description. In practical calculations, however, the basis functions, ϕ's, are written as linear combinations of so-called primitive Gaussians,

$$\phi_\mu = \sum_r d_{\mu r} g_r \tag{2.14}$$

where r represents the type of atomic orbital s, p, d, f ..., $d_{\mu r}$ is a contraction coefficient, and g_r is being termed as a primitive Gaussian, and can be generally expressed in terms of a global coordinate system as

$$g_r = \overline{N}(x - x_A)^l (y - y_A)^m (z - z_A)^n exp(-\alpha r_{iA}^2) \tag{2.15}$$

where l, m, and n are integers which characterize the type or order of the Gaussian function, (x, y, z) are the coordinates of electrons and (x_A, y_A, z_A) represent the nuclear positions, $\overline{N}$ is a normalization factor, and α is the Gaussian exponent. The r_{iA} it is an electron position from center A.[5]

Some of the popular Gaussian basis sets are denoted by 3-21G, 6-31G(d), 6-31+G(d),...etc. The 6-31G(d) and 6-31G(d,p) basis sets are used throughout the present work.

The 3-21G is a split-valence type basis set. The core shells are formed by the linear combination of three Gaussians, and two valence shells, represented by a combination of two and one Gaussian primitives. The 3-21G* basis set was created especially for

the second row elements by the addition of a complete set of six Gaussian primitives.

The 6-31G(d) basis set is a split valence type polarization basis set. The core shells are represented by the linear combination of six Gaussians, and the two valence shells are represented by three and one Gaussian primitives. In addition, six Gaussian primitives are used to describe the polarizability of the non-hydrogen atoms.

The 6-31G(d,p) basis set is constructed the same way as the 6-31G(d), except it contains one set of Gaussian p-type functions to better describe hydrogen atoms and the helium atom.[3]

2.1.5 Hartree-Fock Approximation

As seen earlier, the orbitals may be expanded in terms of a set of basis functions using the expansion coefficients, and the wavefunction can be described as an anti-symmetrized product of molecular orbitals. To find the best possible wavefunction one needs to find the best possible expansion coefficients.

The variational theorem states[3] that, for the lowest electronic state, the expectation value of the energy corresponding to any function Φ can be obtained from the integral

$$E_0 = \int \Phi^* \hat{H} \Phi d\tau \tag{2.16}$$

and it will always be greater than or equal to the exact energy, E, described by the exact wavefunction Ψ,

$$E = \int \Psi^* \hat{H} \Psi d\tau \tag{2.17}$$

As a consequence, the best wavefunction will be the one which gives the lowest possible energy. When selecting a basis set and applying the variational theorem, the coefficients $c_{\mu i}$ from Eq.(2.13) may be adjusted to minimize the expectation value of the energy E_0.

This can be achieved through solution of the Hartree-Fock and Roothaan equations. The method itself is described thoroughly elsewhere,[1–3] and the basic idea is that by minimizing E_0 with respect to the choice of a finite set of spatial orbitals, one can derive the Hartree-Fock equation for closed shell systems of the form

$$\hat{F}(1)\psi_j(1) = \epsilon_j \psi_j(1) \tag{2.18}$$

where $\hat{F}(1)$ is an effective one-electron operator, called the Fock operator, and has the form

$$\hat{F}(1) = -\frac{1}{2}\nabla_1^2 - \sum_A \frac{Z_A}{r_{1A}} + \sum_a (2\hat{J}_a(1) - \hat{K}_a(1)) = \hat{h}(1) + v^{HF}(1) \tag{2.19}$$

The first two terms are forming the core-Hamiltonian operator, $\hat{h}(1)$, and the sum in the last term is a one-electron potential operator called the Hartree-Fock potential, in which the $\hat{J}_a(1)$ and $\hat{K}_a(1)$ are the Coulomb and exchange operators collectively representing all interactions between the electrons, defined as

$$\hat{J}_a(1) = \int \psi_a^*(2) \frac{1}{r_{12}} \psi_a(2) dr_2 \tag{2.20}$$

and

$$\hat{K}_a(1)\psi_i(1) = \left[\int \psi_a^*(2) \frac{1}{r_{12}} \psi_i(2) dr_2 \right] \psi_a(1) \tag{2.21}$$

The substitution of the basis set expansion from Eq.(2.13) into Eq.(2.18), leads to

$$\sum_\nu c_{\nu i} \hat{F}(1) \phi_\nu(1) = \epsilon_i \sum_\nu c_{\nu i} \phi_\nu(1) \tag{2.22}$$

which reduces the problem of finding the Hartree-Fock molecular orbitals to calculating the set of expansion coefficients, $c_{\nu i}$. Multiplication of Eq.(2.22) with ϕ_μ^* and integration gives the matrix equation

$$\sum_{\nu} F_{\mu\nu} c_{\nu i} = \epsilon_i \sum_{\nu} S_{\mu\nu} c_{\nu i} \qquad\qquad i = 1, 2, ..., N \tag{2.23}$$

where ϵ_i is the one-electron energy of molecular orbital ψ_i, $S_{\mu\nu}$ are the elements of the overlap matrix,

$$S_{\mu\nu} = \int \phi_{\nu}^{*}(1)\phi_{\nu}(1)dx_1 dy_1 dz_1 \tag{2.24}$$

and $F_{\mu\nu}$ are the elements of the Fock matrix,

$$F_{\mu\nu} = H_{\mu\nu}^{core} + \sum_{\lambda=1}^{N}\sum_{\sigma=1}^{N} P_{\lambda\sigma}[(\mu\nu|\lambda\sigma) - \frac{1}{2}(\mu\lambda|\nu\sigma)] \tag{2.25}$$

The $H_{\mu\nu}^{core}$ expression is a matrix representing the energy of a single electron in a field of nuclei. It takes the following form:

$$H_{\mu\nu}^{core} = \int \phi_{\mu}^{*}(1)\hat{h}(1)\phi_{\nu}(1)dx_1 dy_1 dz_1, \tag{2.26}$$

The $P_{\lambda\sigma}$ term stands for the elements of the one-electron density matrix,

$$P_{\lambda\sigma} = 2 \sum_{i}^{occupied} c_{\lambda i}^{*} c_{\sigma i} \tag{2.27}$$

The quantities $(\mu\nu|\lambda\sigma)$ are the two-electron repulsion integrals and have the form

$$(\mu\nu|\lambda\sigma) = \int\int \phi_\mu^*(1)\phi_\nu(1)\frac{1}{r_{12}}\phi_\lambda^*(2)\phi_\sigma(2)dr_1dr_2 \tag{2.28}$$

In the end, the sum of the electronic energy and nuclear repulsion energy expression will yield the total energy

$$E_{HF} = \frac{1}{2}\sum_{\mu=1}^{N}\sum_{\nu=1}^{N} P_{\mu\nu}(F_{\mu\nu} + H_{\mu\nu}^{core}) + V_{NN} \tag{2.29}$$

Roothaan's equation[6] can be formulated as a single matrix equation,

$$Fc = Sc\epsilon \tag{2.30}$$

where c is the N x N square matrix of the expansion coefficients $c_{\nu i}$

$$C = \begin{pmatrix} c_{11} & c_{12} & \cdots & c_{1N} \\ c_{21} & c_{22} & \cdots & c_{2N} \\ . & . & & . \\ . & . & & . \\ . & . & & . \\ c_{N1} & c_{N2} & \cdots & c_{NN} \end{pmatrix} \tag{2.31}$$

and ϵ is a diagonal matrix of the orbital energies ϵ_i,

$$\epsilon = \begin{pmatrix} \epsilon_1 & & & \\ & \epsilon_2 & & \mathbf{0} \\ & & . & \\ & \mathbf{0} & & \\ & & & . \\ & & & \epsilon_N \end{pmatrix} \tag{2.32}$$

Solving the matrix equation (2.30) is done through an iterative process, called the self-consistent-field (SCF) procedure.[1] The procedure starts with the specification of the coordinates of the molecule and the basis set. After this, all required molecular integrals, the overlap, one-electron and two-electron integrals are calculated and an

initial guess for the density matrix is obtained.

This initial set is used to compute the Fock matrix, which further will give an initial set of orbital energies ϵ_i's. The orbitals are then used to solve Roothaan's equation for an improved set of coefficients, giving an improved set of molecular orbitals, which are used to compute an improved Fock matrix.

The calculations are continued until no further improvement in molecular orbital coefficients and energies occur from one iteration to the next. Usually the iteration terminates on the convergence of the density matrix. Convergence means that the last two calculated values should differ by no more than the quantity representing the convergence criteria specified in the beginning of the iteration.

2.2 Post Hartree-Fock Methods

In the Hartree-Fock approximation, there is an incomplete description of the total energy of a system, because electrons with opposite spins are not correlated. If the exact energy of a system can be defined[3] as the sum

$$E_{exact} = E_{HF} + E_{corr} \tag{2.33}$$

the correlation energy is the difference between the Hartree-Fock energy and the exact (nonrelativistic) energy. Correlation energy can be described using the so called

Post Hartree-Fock methods, like configuration interaction, coupled-cluster or perturbation theory. They are all well documented[1, 3] and are based on multideterminantal wavefunctions.

2.2.1 Møller-Plesset Perturbation Theory

According to the Møller-Plesset perturbation theory,[3] an electronic Hamiltonian can be formulated as the sum of the zeroth order Hamiltonian, $\hat{H}_0$, represented by the sum of the one-electron Fock operators, and a perturbation $\lambda\hat{V}$

$$\hat{H}_\lambda = \hat{H}_0 + \lambda\hat{V} \tag{2.34}$$

The perturbation, $\lambda\hat{V}$, can be written as

$$\lambda\hat{V} = \lambda(\hat{H} - \hat{H}_0), \tag{2.35}$$

where $\hat{H}$ is the correct Hamiltonian and λ is a dimensionless parameter. The energy of the system can be expanded in powers of λ as,

$$E_\lambda = E^{(0)} + \lambda E^{(1)} + \lambda^2 E^{(2)} + ... \tag{2.36}$$

The existing perturbation methods can be achieved by truncation of the series in Eq.(2.36) to various orders. MP2 means truncation after second order, MP3 after third order and so on.

2.3 Density Functional Theory

2.3.1 Electron Density

In an atomic or molecular system, the electron density is the amount of electronic charge within the unit volume[7] and it can be defined as the following multiple integral over the spin coordinates of all electrons

$$\rho(\mathbf{r}_1) = n \int \dots \int |\Psi(x_1, x_2, \dots, x_n)|^2 \, ds_1 dx_2 \dots dx_n \tag{2.37}$$

Integrating over all space it gives the total number of electrons

$$\int \rho(\mathbf{r}) d\mathbf{r} = n \tag{2.38}$$

2.3.2 Hohenberg-Kohn Equations

An alternative method which uses the electron density instead of the wavefunction to express a system's energy, is called density functional theory.[7–9]

It was shown[10] that the external potential present in the Hamiltonian (Eq.(2.5)) is determined by the electron density $\rho(\mathbf{r})$, and from Eq.(2.38), it can be seen that ρ also determines the number of electrons. As has been shown later for all molecules

without artificial boundaries, any positive volume part of the electron density determines all other properties including energy.[11]

There is an exact energy functional $E[\rho]$, which can describe the energy of the entire atomic or molecular system in terms of the density, having the form

$$E[\rho] = V_{ne}[\rho] + F_{HK}[\rho] \tag{2.39}$$

where V_{ne} is the potential energy due to the nucleus-electron attraction,

$$V_{ne}[\rho] = \sum_{A}^{M} \int \frac{Z_A}{|r - r_A|} \rho(r) dr \tag{2.40}$$

and $F_{HK}[\rho]$ is the sum of kinetic and electron-electron interaction term,

$$F_{HK}[\rho] = T[\rho] + V_{ee}[\rho] \tag{2.41}$$

and is called the Hohenberg-Kohn universal functional. The repulsion energy, $V_{ee}[\rho]$, can further be written as

$$V_{ee}[\rho] = \frac{1}{2} \int \int \frac{\rho(r_1)\rho(r_2)}{|r_1 - r_2|} dr_1 dr_2 \tag{2.42}$$

The same theorem[10] states that the energy functional, $E[\rho]$, for the true ground state

density ρ, will give the ground state energy E_0 of the system, and by applying the variational principle for any trial density $\tilde{\rho}$, the following relation holds

$$E_0 \leq E[\tilde{\rho}] \tag{2.43}$$

2.3.3 Kohn-Sham Equations

For a better description of the $F_{HK}[\rho]$ expression, Kohn and Sham rewrote[12] Eq.(2.41) as the sum

$$F_{HK}[\rho] = T_S[\rho] + J[\rho] + E_{XC}[\rho] \tag{2.44}$$

where $J[\rho]$ represents the classical Coulomb repulsion, T_S is the kinetic energy of all non-interacting electrons of a fictitious reference system with the same density as the real one expressed using the so-called Kohn-Sham (KS) orbitals, φ_i

$$T_S = -\frac{1}{2}\sum_i^N \left\langle \varphi_i | \nabla^2 | \varphi_i \right\rangle \tag{2.45}$$

and E_{XC} is an exchange-correlation energy which can be defined as

$$E_{XC}[\rho] = \Delta T[\rho] + \Delta V_{ee}[\rho] \tag{2.46}$$

The non-interacting kinetic energy is not equal to the true kinetic energy of a system so the exchange-correlation term, E_{XC} is being represented as a sum of the difference between the true and the non-interacting kinetic energies and the difference between the classical and the non-classical electrostatic contributions. After the inclusion of these additional terms the expression for the energy in terms of density becomes

$$E[\rho] = V_{ne}[\rho] + T_S[\rho] + J[\rho] + E_{XC}[\rho] \tag{2.47}$$

Similar to the way in which the Hartree-Fock approximation minimizes the energy with respect to the choice of orbitals φ, one can derive the Kohn-Sham equations[12]

$$H_i^{KS}\varphi_i = \epsilon_i\varphi_i \tag{2.48}$$

where H_i^{KS} is the KS operator defined as

$$H_i^{KS} = -\frac{1}{2}\nabla_i^2 - \sum_A^M \frac{Z_A}{|r_i - r_A|} + \int \frac{\rho(r')}{r_i - r'}dr' + V_{XC} \tag{2.49}$$

and

$$V_{XC} = \frac{\delta E_{XC}}{\delta \rho} \tag{2.50}$$

is the functional derivative of E_{XC} with respect to density. Analogous to the HF self-consistent field method, one can also solve the Kohn-Sham equations iteratively. The method is described thoroughly in the literature.[7–9]

In general, the major difference between the two theoretical approaches (*ab initio* and DFT) lies in the approximations made. In the *ab initio* (Hartree-Fock) method, the approximation is introduced from the beginning, meaning that it will never give an exact solution. DFT could give the exact solution if one did not need to approximate the exchange and correlation terms. The most common approximate exchange correlation functionals can be classified as follows: the ones based on the early local density approximations, gradient corrected functionals, and hybrid functionals.

The gradient corrected functionals are usually a combination of a gradient corrected exchange functional and a gradient corrected correlation functional, BLYP for example, refers to Becke's corrected exchange functional[13] in combination with the Lee, Yang, Parr correlation functional.[14]

Hybrid functionals, however, also incorporate an exact Hartree-Fock exchange functional in the usual density based approximation. B3LYP is one of the most popular hybrid exchange-correlation functional, having the form[15]

$$E_{XC}^{B3LYP} = (1-a)E_X^{LDA} + aE_X^{HF} + bE_X^{B88} + cE_C^{LYP} + (1-c)E_C^{VWN3} \qquad (2.51)$$

where LDA stands for local density approximation, VWN3 for the Vosko, Wilk, Nusair local correlation functional,[16] B88 is Becke's corrected exchange functional,[13] LYP is the above mentioned correlation functional, and E_X^{HF} is the Hartree-Fock local exchange. The empirical parameters a, b, and c were determined by fitting to the atomization energies, ionization potentials, proton affinities and first-row atomic energies, and have the values 0.20, 0.72, and 0.81 respectively.[15]

2.4 Geometry Optimization

2.4.1 Equilibrium Geometry

Self-consistent field calculations at many geometries with different nuclear arrangements in order to minimize the energy of a system result in an equilibrium geometry. The energy is a function of the nuclear coordinates, and can define the potential-energy surface (PES) of the molecule. The entire process is also called geometry optimization and there are many algorithms which are used to find the local minimum energy. The most efficient methods to obtain an equilibrium geometry are those which perform repeated calculations of both the total energy and its derivatives.[2] The partial derivatives of the energy can be described as a vector called the energy gradient. At a local minimum, the gradient must be zero. At any point on the

PES where the gradient is zero, one finds a stationary point which can be a minimum, a maximum, or a saddle point (if nondegenerate).

In this study, the goal was to find the energy minimum of the structures under investigation. To be sure that the optimized geometry is a true minimum on the PES, the second derivatives of the energy must be calculated at the same geometry. This is verified by performing frequency calculations.

2.4.2 Vibrational Frequencies

The harmonic vibrational frequencies of a molecule can be calculated theoretically.[3] The classical vibrational energy of the molecule having N number of atoms near the equilibrium structure can be written as

$$E = \frac{1}{2}\sum_{i=1}^{3N} \dot{q}_i^2 + V(q) \tag{2.52}$$

where the first term represents the vibrational kinetic energy in terms of mass adjusted coordinates, and $V(q)$ is the potential energy, which can be written as an expansion in terms of Taylor series (here truncated at second-order)

$$V(q) = V(q_{eq}) + \frac{1}{2!}\sum_i \sum_j \left(\frac{\partial^2 V}{\partial q_i \partial q_j}\right)_{eq} q_i q_j \tag{2.53}$$

where $V(q_{eq})$ represents the potential energy at the equilibrium configuration. The

q_i represents the mass weighted Cartesian displacements, defined as

$$q_i = M_i^{\frac{1}{2}}(x_i - x_{i,eq}) \tag{2.54}$$

where x_i represents the locations of the nuclei relative to their equilibrium positions $x_{i,eq}$ and their masses M_i.

From the second derivatives of the potential energy in Eq. 2.53, the mass weighted force constants, f_{ij} can be formed

$$f_{ij} = \left(\frac{\partial^2 V}{\partial q_i \partial q_j}\right)_{eq} \tag{2.55}$$

The force constants can be evaluated analytically or by single numerical differentiation of analytical first derivatives,

$$\frac{\partial^2 V}{\partial q_i \partial q_j} \simeq \frac{\Delta(\partial V/\partial q_j)}{\Delta q_i} \tag{2.56}$$

or by double numerical differentiation,

$$\frac{\partial^2 V}{\partial q_i \partial q_j} \simeq \frac{\Delta(\Delta V)}{\Delta q_i \, \Delta \, q_j} \tag{2.57}$$

In the actual calculations, especially for polyatomic systems, the f_{ij} are the elements

of a force constant matrix, which can be diagonalized, and its eigenvalues, λ_i, will give the actual values for force constants, which can be used to estimate the frequencies as

$$\nu_i = \frac{1}{2\pi}\sqrt{\lambda_i} \tag{2.58}$$

Positive force constants are a sign that moving out from the equilibrium zone results in an increase in energy. Thus having positive frequencies implies a true minimum on the PES. There are cases where negative force constants are present which can lead to the existence of imaginary frequencies. One imaginary frequency means that, on the potential energy surface (PES) of the molecule, there is a minimum in all dimensions but one. This is also called a first order saddle point or transition state.

2.4.3 Zero-Point Vibrational Energy

A nonlinear molecule containing N atoms has a total of $3N$ - 6 vibrational degrees of freedom. The vibration of molecules is most often described using the harmonic oscillator approximation. In this approximation, the vibrational energy of a molecule containing N atoms is the sum of $3N$ - 6 normal mode vibrations.

The vibrational energy of a molecule at absolute zero (0 K) is called zero-point vibrational energy (ZPVE), and is given by

$$E_{ZPVE} = \frac{1}{2}h\sum_{i}^{3N-6}\nu_i \tag{2.59}$$

where ν_i is a normal mode vibrational frequency. The value of the zero-point vibrational energy is usually added to the total energy of the optimized molecule, for a more accurate description of the total energy of a system.

2.5 Molecular Shape

The representation of the shape of the molecules varies from simple ones, such as ball and stick, ball and bond type, and tube or wireframe representions to more complex surface type representations based on a specific property, *e.g.* electron density surfaces, electrostatic potential surfaces, solvent accessible surfaces, or van der Waals surfaces.

This thesis uses electron density as a theoretically calculated property to represent the shape of the molecules of interest.

2.5.1 Molecular Isodensity Contours

The electron density $\rho(\mathbf{r})$ can be calculated from the n-electron wavefunction solution of the electronic Schrödinger equation from Eq.(2.37). For a single-determinantal

wavefunction in which the orbitals are expanded in terms of a set of N basis functions, ϕ_μ, the electron density is given by the expression,[3]

$$\rho(\mathbf{r}) = \sum_{\mu}^{N} \sum_{\nu}^{N} P_{\mu\nu} \phi_\mu \phi_\nu \tag{2.60}$$

where $P_{\mu\nu}$ are the elements of the density matrix, obtained from the eigenfunctions of the electronic Hamiltonian,

$$P_{\mu\nu} = 2 \sum_{i}^{N/2} c_{\nu i} c_{\mu i}^{*} \tag{2.61}$$

The information on the electronic density gained through electronic structure calculations can be used for further analysis regarding the shape of a molecule.

The shape group method[17] offers a comprehensive description of the shapes of molecules. It uses the concept of a molecular isodensity contour (MIDCO) surface, which plays an important role in the description of three dimensional electron densities. Accordingly, for any nuclear configuration, by choosing a small value a for the electron density, and by selecting all those points $\mathbf{r}$ in the three dimensional space where the density $\rho(\mathbf{r})$ is equal with the value of a (in other words, the electron density is constant) a molecular surface $G(a)$ can be defined as

$$G(a) = \{\mathbf{r} : \rho(\mathbf{r}) = a\} \tag{2.62}$$

At very high density, there are disconnected, isolated spherical regions around the nuclei. As the density decreases, the isolated regions are connected, revealing existing bonding patterns. At very low density, the surface becomes large enough to enclose the entire set of nuclei.

2.6 Isomerism

Molecules having the same molecular formula but different structures are called isomers. They can be constitutional (structural) isomers or stereoisomers.

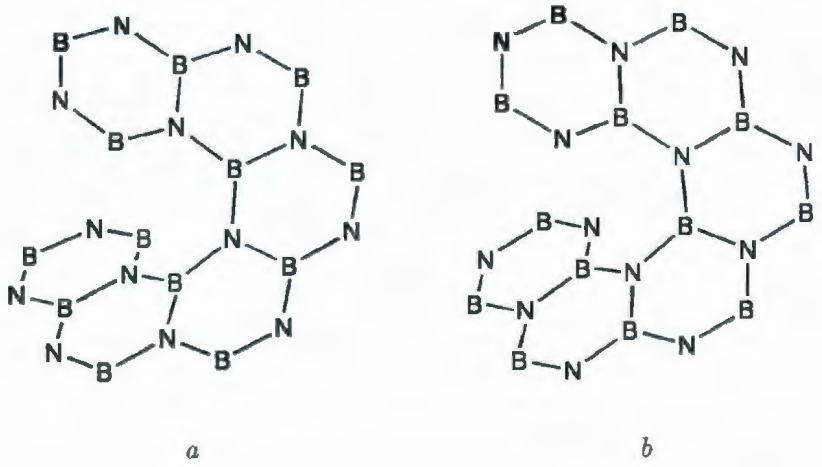

a *b*

Figure 2.1: Example of angular isomerism in helices with 6 fused units (*a* and *b*)

During the present study, a particular kind of isomerism was observed in some of

the helices studied. That is, in the helices formed by an even number of fused units, the alternation of boron and nitrogen atoms leads to angular isomerism.

For example, if one takes structure *a* from Figure 2.1 containing six fused hexagonal units and alternates the position of the boron and nitrogen atoms in the helices, one gets a different structure *b*.

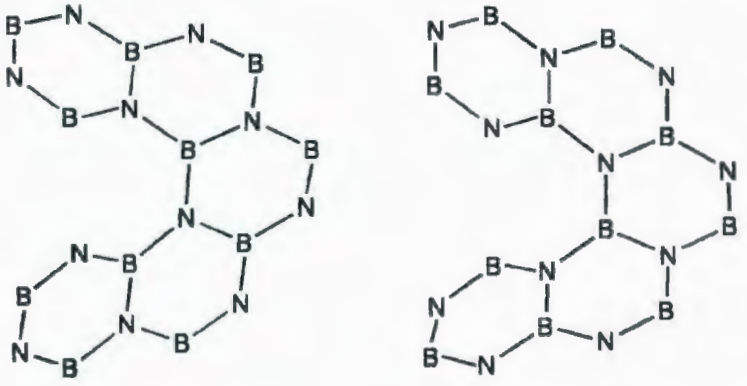

c *d*

Figure 2.2: Example of nonisomerism in helices with 5 fused units (*c* and *d*)

Taking the helix *c* from Figure 2.2 containing an odd number (five) of fused units and switching the boron and nitrogen atoms gives the same structure, *d*. As can be seen, there is no isomerism present in the case of odd numbers of fused rings; one structure is simply rotated by 180 degrees around an imaginary horizontal axis situated in the middle of the helix, becoming identical to the other.

More complicated possibilities exist if further rings are used to extend such helices laterally.

2.7 Computational Details

As with all other theoretical and experimental studies, the calculations and results presented in this thesis are not exempt from sources of error.

The capabilities of the Hartree-Fock approximation in describing the correct ground state is restricted due to the HF limit problem and the fact that this level of theory does not account for the electron correlation.[3] To better describe the structure of the helices studied, geometry optimization was also performed with density functional theory which is based on the electron density and accounts for some of the correlation energy.

Geometry optimization of all the structures was done at the *ab initio* and DFT levels of theory using medium size basis sets 6-31G(d) and 6-31G(d,p). Single point energy calculations using second-order Møller-Plesset (MP2) perturbation theory were also performed. All three levels of theory HF, B3LYP, and MP2 showed the same trend in the energy changes in case of the studied isomers.

Similar basis sets and levels of theory were also used in some recent studies[18–21] on boron-nitrogen structures containing fused borazine rings. One of the studies[18] focused on the boron-nitrogen analogue of naphthalene. These studies have compared theoretical data obtained at 6-31G(d) and 6-31+G(d) basis sets. They reported negligible improvement using the higher basis set and suggested the smaller sized 6-31G(d) basis set as being resonable for systems containing boron and nitrogen. Furthermore, while the calculated bond lengths at HF level were in good agreement with the ex-

perimental values, the ones calculated at the MP2 level of theory overestimated the experimental bond lengths.

Due to this fact and the large size of some of the helices studied in this thesis, geometry optimization at the MP2 level was avoided. It was decided that single point energy calculations at the MP2 level of theory using the 6-31G(d) basis set on the series of angular isomers would suffice in the description of their relative energies. However, a preliminary geometry optimization was still performed at MP2/6-31G(d) level of theory on the boron-nitrogen [6]helicene with no effect on the overall helical geometry. Data on the lowest vibrational frequencies and ground state energy at the MP2 level of theory is provided in Appendix D.

Throughout the thesis, the flexibility and spring-like behaviour of the studied helical systems was emphasised. This is justified by the values of the normal modes. Since these molecules do have the actual shape of a spring, one can expect that their vibrational motions imitate the vibration motions of macroscopic springs. Visualisation of the lowest vibrational frequencies for some of the helices is depicted in Appendix C.

Overall, within the levels of theory and basis sets used, the results presented in this thesis are able to describe the electronic structure and demonstrate the relative stability of the isomeric helical systems.

Bibliography

[1] A. Szabo and N. S. Ostlund. *Modern Quantum Chemistry.* Dover Publications, Inc., New York, 1996.

[2] I. N. Levine. *Quantum Chemistry.* Prentice-Hall, Inc., New Jersey, 2000.

[3] W. J. Hehre, L. Radom, P. v.R. Schleyer, and J. A. Pople. *Ab Initio Molecular Orbital Theory.* John Wiley and Sons, Inc., New York, 1986.

[4] J.C. Slater. *Phys. Rev.*, 38:1109, 1931.

[5] D. B. Cook. *Handbook of Computational Quantum Chemistry.* Oxford University Press, Inc., New York, 1999.

[6] C. C. J. Roothaan. *Rev. Mod. Phys.*, 23:69, 1951.

[7] R. G. Parr and W. Yang. *Density-Functional Theory of Atoms and Molecules.* Oxford University Press, Inc., New York, 1989.

[8] W. Koch and M. C. Holthausen. *A Chemist's Guide to Density Functional Theory.* Wiley-VCH Verlag GmbH, Weinheim, 2001.

[9] J. K. Labanowski and J. W. Andzelm. *Density Functional Methods in Chemistry.* Springer- Verlag, New York, 1991.

[10] P. Hohenberg and W. Kohn. *Phys. Rev.*, 136(3B):864, 1964.

[11] P. G. Mezey. *Mol. Phys.*, 96:169, 1999.

[12] P. Hohenberg and W. Kohn. *Phys. Rev.*, 140(4A):1133, 1965.

[13] A. D. Becke. *Phys. Rev. A*, 38:3098, 1988.

[14] C. Lee, W. Yang, and R.G. Parr. *Phys. Rev. B*, 37:785, 1988.

[15] J. B. Foresman and Æ. Frisch. *Exploring Chemistry with Electronic Structure Methods.* Gaussian, Inc., Pittsburgh, 1996.

[16] S. H. Vosko, L. Wilk, and M. Nusair. *Canadian J. Phys.*, 58:1200, 1980.

[17] P. G. Mezey. *Shape in Chemistry.* VCH Publishers, Inc., New York, 1993.

[18] T. Kar, D. E. Elmore, and S. Scheiner. *J. Mol. Struct.(THEOCHEM)*, 392:65, 1997.

[19] T. Kato and T. Yamabe. *J. Chem. Phys.*, 118:3804, 2003.

[20] H. Wang, H. S. Wu, and J. F. Jia. *Chin. J. Chem.*, 24:731, 2006.

[21] C. J. Johnson and R. W. Zoellner. *J. Mol. Struct.(THEOCHEM)*, 893:9, 2009.

Chapter 3

Theoretical study on the structure and stability of some unusual boron-nitrogen helices *

3.1 Introduction

The interest in the structure, bonding, and electronic properties of boron-nitrogen clusters has increased in recent years.[1–4] The boron-nitrogen atom pair, being isoelectronic with the carbon-carbon atom pair, has been a likely replacement of the latter in a variety of carbon-based compounds. The change in nuclear charges introduces several specific effects in the structure as well as the electronic properties, which pro-

*Adapted from: C. E. Szakacs and P. G. Mezey. *J. Phys. Chem. A*, 112(11):2477, 2008.

vide new options for interesting molecular systems and potential nanomaterials.

The discovery of hexahelicene[5] encouraged investigations towards helically extended π systems leading, for example, to the synthesis[6] of helical [7]phenylene. These structures are angular systems formed from N fused benzene rings in the case of helicenes and N fused benzene rings with N-1 interposed cyclobutadiene rings in the case of phenylenes. Additional interest has been generated by their unusual chirality and optical properties.[7, 8] The geometry and energetics of phenylenes, helicenes and their isomers have been the subject of numerous theoretical studies.[9–12] Most recently,[13] theoretical investigations were carried out on the stability of more extended systems, up to double turn polyhelicenes, polyphenylenes, and analogous structures, as potential precursors towards helical graphites.

Borazine,[14] the boron-nitrogen analogue of benzene, is well known. Borazanaphthalene, the boron-nitrogen analogue of naphthalene, first observed as a product formed during the gas-phase pyrolysis of borazine[15] has also been characterized both experimentally[16–18] and theoretically.[19] An earlier study investigated molecules containing three fused borazine rings,[20] suggesting a possibility for the existence of boron-nitrogen polymers containing larger number of rings. Further studies reported on the stability of boron-nitrogen cyclacenes[21] which are belt-like structure analogues of the carbon based cyclacenes. A series of linearly annulated boron-nitrogen analogues of acenes were also subject of detailed density functional calculations.[22] Most recently,[23] the synthesis of a tubular conical BN helix structure, having elastic properties has

been reported. Helical all-nitrogen and helical nitrogen rich fused-ring clusters were studied as well,[24] however, to our knowledge, boron-nitrogen analogues of the helicenic and phenylenic angular systems were not yet the subject of any detailed theoretical studies.

In the present chapter, computational investigations are reported for a series of single and double turn boron-nitrogen analogues of [N]helicenes and their angular isomers (possible only if N is an even number), [N]phenylenes, and [N]methylenylnaphthalenes. The boron-nitrogen analogues of benzene **a**, cyclobutadiene **b**, and methylenylnaphthalene **c**, are the structural units of these angular systems. N fused **a** rings

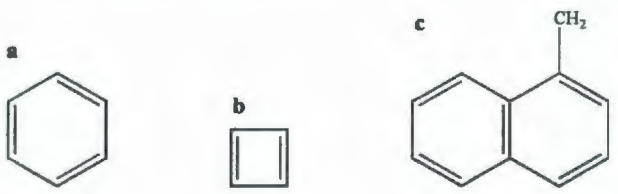

Figure 3.1: Structural units of the helices

form the single turn ($N = 5$, 6, and 7) and double turn ($N = 12$) versions of the boron-nitrogen analogues of [N]helicenes. An even number of rings in the boron-nitrogen helicenes leads to the existence of angular isomers, which can be distinguished by the different arrangements of the B and N atoms in the terminal ring (Figure 3.2). For brevity, the **d** isomer will be denoted as **BN** and the **e** isomer as **NB**. The boron-nitrogen analogues of [N]phenylenes are comprised of N ($N = 5$, 6, 7, and 13)

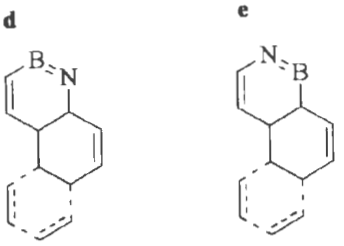

Figure 3.2: The two possible structures **d, e** in the case of helicenes with even *N* rings, where the B and N atoms, one of them present at each vertex of these structural formulas, are shown only along one bond.

alternating **a** units fused to *N*-1 **b** units. Finally the helical boron-nitrogen analogue of [6]polymethylenylnaphthalene is obtained with six fused **c** units.

3.2 Computational methodology

The structures **1 - 8** (Figure 3.3 and Figure 3.4) were optimized at two different levels of theory, Hartree-Fock and DFT with the B3LYP functional, using the 6-31G(d) basis set.[25, 26] All these methods are implemented in the Gaussian 03 software package.[27] For all optimized geometries, harmonic vibrational frequencies were computed at the same level of theory. The lowest vibrational frequencies for all the optimized structures, no imaginary frequencies among them, are shown in Table 3.1. Single point energy calculations were performed at the MP2 level of theory using the 6-31G(d) basis set for isomeric helices with HF optimized geometries.

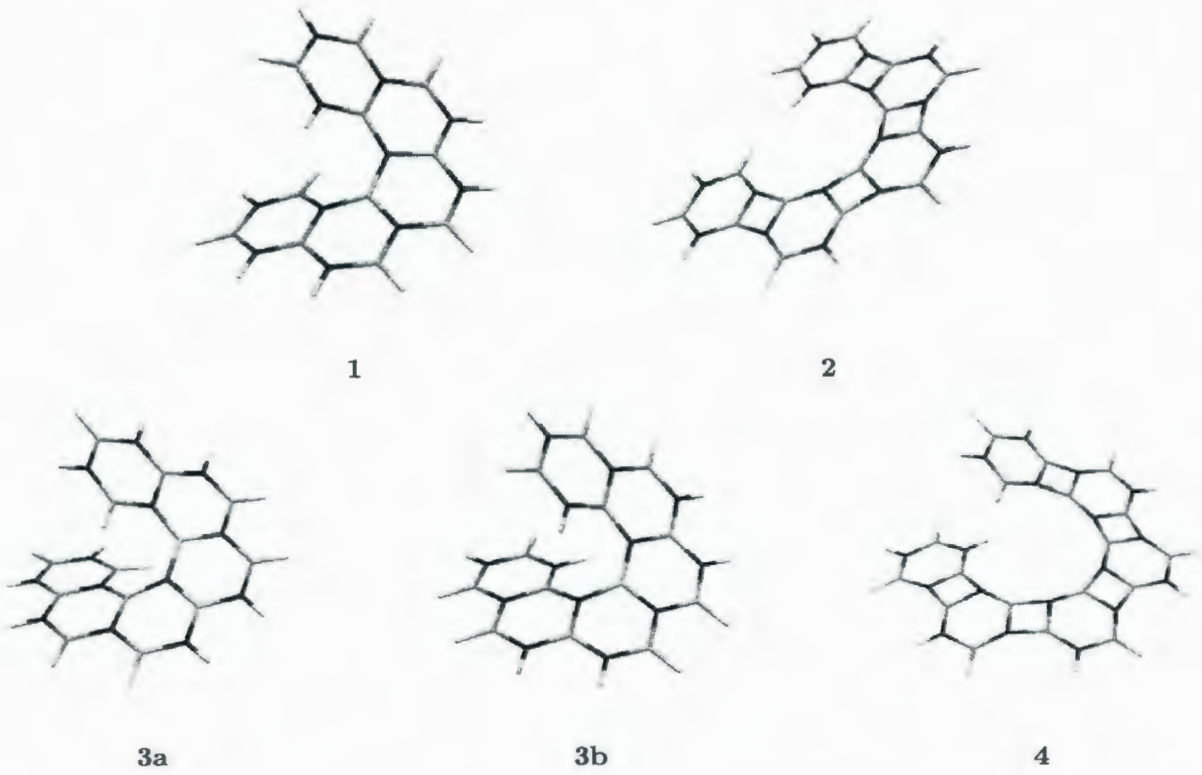

Figure 3.3: The optimized geometries of boron-nitrogen analogues of [*N*]helicenes and [*N*]phenylenes, **1-4** (the boron atoms are in light, the nitrogen atoms are in dark colour)

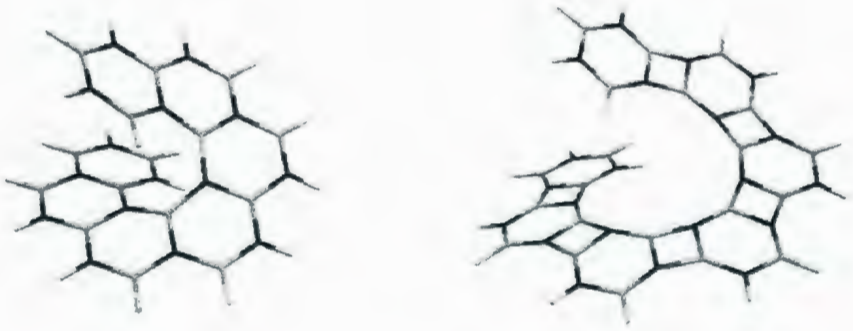

5 6

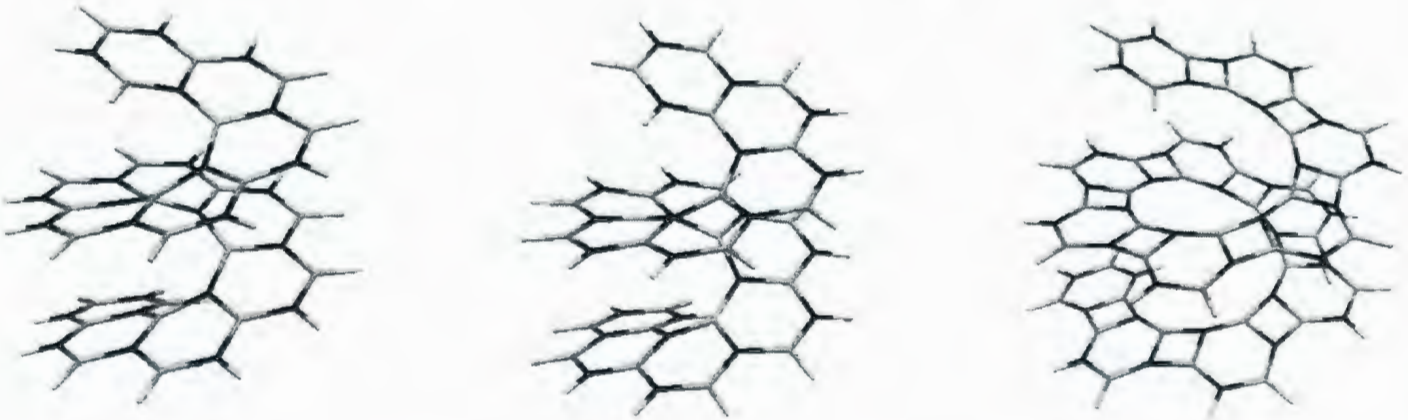

7a 7b 8

Figure 3.4: The optimized geometries of boron-nitrogen analogues of [*N*]helicenes and [*N*]phenylenes, **5-8**

Table 3.1: The lowest wavenumbers (cm^{-1}) of the studied boron-nitrogen helices. (Calculated values at HF/6-31G(d) shown in the second column, followed by those at B3LYP/6-31G(d) in the third column)

BN[5]helicene, **1**	47.19	45.58
BN[6]helicene, **3a**	34.27	31.96
NB[6]helicene, **3b**	31.94	32.44
BN[7]helicene, **5**	32.01	26.76
BN[12]helicene, **7a**	39.15	34.41
NB[12]helicene , **7b**	37.51	36.58
BN[5]phenylene, **2**	18.17	19.69
BN[6]phenylene, **4**	19.57	16.44
BN[7]phenylene, **6**	14.72	12.66
BN[13]phenylene, **8**	13.36	11.51
BN[6]methylenylnaphthalene, **9a**	15.88	15.41
NB[6]methylenylnaphthalene, **9b**	16.64	13.08

In order to investigate the bonding pattern in the systems, electron density analysis was performed at the HF/6-31G(d) level.

3.3 Results and Discussions

Geometries of the optimized structures are presented in Figure 3.3 and Figure 3.4, and the bond lengths in the single turn boron-nitrogen helices are indicated in Figure 3.5, 3.6, and 3.7.

	BN	NB
a =	1.418-1.419	1.418
b =	1.434-1.437	1.433-1.438
c =	1.450-1.457	1.452-1.456
d =	1.454-1.457	1.456-1.460

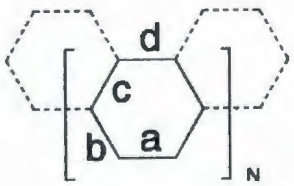

Figure 3.5: Calculated bond lengths (in Ångströms) of **BN**[6]helicene and **NB**[6]helicene at HF/6-31G(d)

Investigations on the optimized structures of **1**, **3a**, **3b**, **5**, **7a**, and **7b**, the boron-nitrogen analogues of [N]helicenes (N = 5, 6, 7, and 12), confirmed the existence of local energy minima by having real vibrational frequencies at both the Hartree-Fock

and DFT levels with the 6-31G(d) basis set.

a = 1.446-1.448

b = 1.414-1.417

c = 1.472-1.476

d = 1.394-1.400

e = 1.455-1.456

f = 1.446-1.449

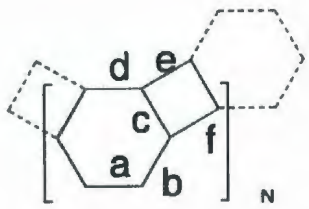

Figure 3.6: Calculated bond lengths (in Ångströms) of **BN**[6]phenylene at HF/6-31G(d)

Noted with **a**, **b**, **c** and **d** in Figure 3.5 are the bond lengths of the boron-nitrogen analogue of helicenes found for the nonterminal rings of the helical systems. These bonds appear longer than those in their reported carbon analogues,[13] which could result from the weakening of the π bonding in the boron-nitrogen ring, due to the electronegativity difference between the boron and the nitrogen atoms.

	BN	NB
a =	1.418-1.419	1.418-1419
b =	1.429-1.441	1.428-1442
c =	1.445-1.452	1.446-1450
d =	1.439-1.440	1.439-1441
e =	1.444-1.448	1.445-1451
f =	1.454-1.455	1.456-1457

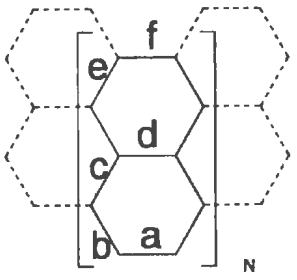

Figure 3.7: Calculated bond lengths (in Ångströms) of **BN**[6]methylenylnaphthalene and **NB**[6]methylenylnaphthalene at HF/6-31G(d)

However, these distances still fall in the range of the experimentally determined bond length values (1.400 to 1.453 Å) of borazanaphtalene,[18] which could be considered a simple model somewhat similar to these fused helical systems. The bonding pattern appears to be stable and nearly uniform, with stronger bonds on the peripheries of the rings (bond type **a** in Figure 3.5), that is justified by general electron repulsion effects: electrons seek the periphery of extended structures, allowing them to increase

their formal "mutual distances".

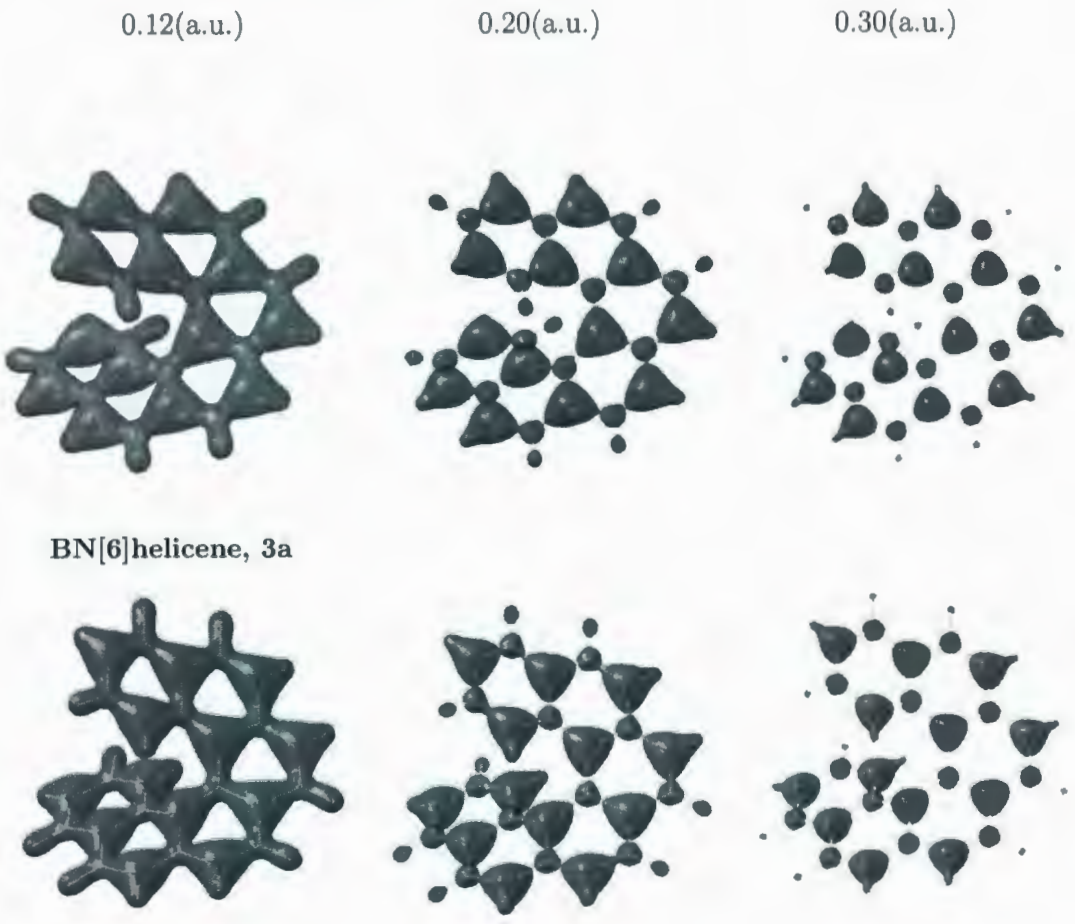

Figure 3.8: Electron density isocontours of single turn boron-nitrogen helicenes

This is in agreement with the results of more detailed electron density shape analysis of these molecules (Figure 3.8). The isocontours at the high density value 0.30 a.u. already show significant deformations from local spherical shape of the constituent

atoms.

Table 3.2: Total energies, at HF and DFT (in Hartree) and single point energies at MP2 (in Hartree) in case of boron-nitrogen analogues of [N]helicenes

Molecule	Level/Basis set		
	HF/6-31G(d)	B3LYP/6-31G(d)	MP2/6-31G(d)
BN[5]helicene, **1**	-879.7494	-885.1388	
BN[6]helicene, **3a**	-1039.3953 (3.5)*	-1045.7518 (4.1)	-1042.4254 (3.7)
NB[6]helicene, **3b**	-1039.4009 (0.0)	-1045.7584 (0.0)	-1042.4313 (0.0)
BN[7]helicene, **5**	-1199.0472	-1206.3717	
BN[12]helicene, **7a**	-1997.2850 (4.3)	-2009.4474 (4.8)	-2003.1411 (4.5)
NB[12]helicene , **7b**	-1997.2919 (0.0)	-2009.4550 (0.0)	-2003.1482 (0.0)

*The values in parenthesis show the energy in kcal/mol of the BN isomers, relative to the NB isomers in the case of $N = 6$ and $N = 12$.

At the isocontour value of 0.20 a.u., the electron density analysis confirms bond type **a** being the strongest. The 0.12 a.u. electron density contours are special. On the one hand, they show a level of electron density where a single, but multiply-connected contour presents a prominent alteration of electron rich and electron deficient atoms. On the other hand, one can notice a rare phenomenon: actual hexagonal local structures give rise to nearly perfect triangular holes, a feature that may be useful in "shape-tuning" of local interactions. Considering an approaching molecule, interac-

tions occurring at high density are effected by hexagonal patterns, while low density interactions are effected by triangular patterns.

Taking into consideration the number of rings, as N increases, a decrease in the total energy of unit structures is observed at both levels of theory (Table 3.2). The gradual energy changes from molecule to molecule are approximately -159.65 and -160.61 $\pm$ 0.01 Hartrees at the HF/6-31G(d) and the B3LYP/6-31G(d) levels, respectively. In case of an even number of N rings, both in the single **3** and double helix **7**, the **NB** isomers **3b** and **7b** are energetically more stable than their **BN** counterparts. The difference in the relative energy values between the two isomers is 3.5, 4.1, and 3.7 kcal/mol for single-turn helix and 4.3, 4.8, and 4.5 kcal/mol for double-turn helix, at the HF/6-31G(d), B3LYP/6-31G(d), and MP2/6-31G(d)//HF/6-31G(d), respectively.

Table 3.3: Total energies (in Hartree) of boron-nitrogen analogues of [N]phenylenes

Molecule	Level/Basis set	
	HF/6-31G(d)	B3LYP/6-31G(d)
BN[5]phenylene, **2**	-1196.5797	-1203.8299
BN[6]phenylene, **4**	-1435.4344	-1444.1177
BN[7]phenylene, **5**	-1674.2915	-1684.4076
BN[13]phenylene, **8**	-3107.4371	-3126.1526

The boron-nitrogen analogues of [N]phenylenes **2, 4, 6**, and **8**, were also optimized and found to be energy minimum structures, confirmed by vibrational frequency calculations. Except for BN[5]phenylene, which has a planar structure, all the others have helical geometries (Figure 3.3 and Figure 3.4). The unit structures in all species are characterized by six B-N bond lengths, noted with **a, b, c, d, e**, and **f** in Figure 3.6.

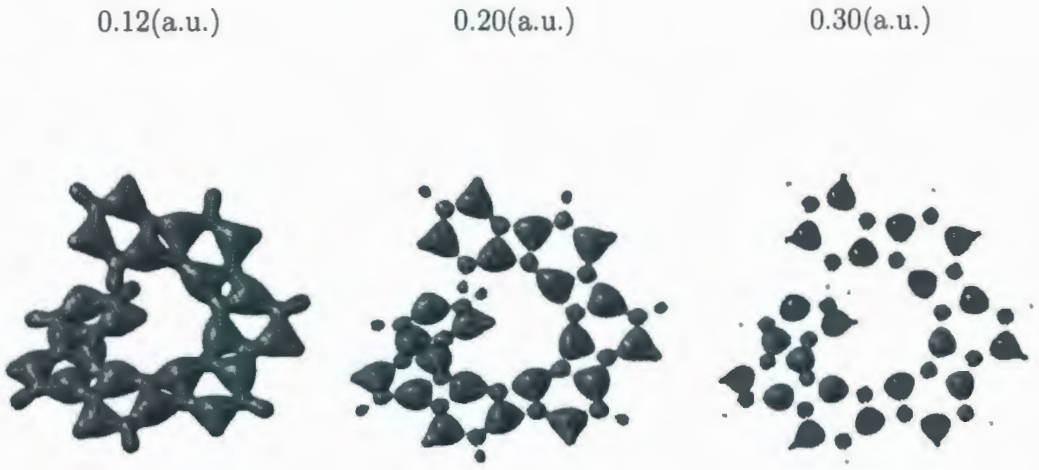

Figure 3.9: Electron density isocontours of single-turn BN[7]phenylene

In the helices **4, 6**, and **8**, the bond lengths are ranging from 1.394 to 1.476 Å, where bond types **d**(1.394-1.400 Å) and **b**(1.414-1.417 Å) have a prominent double bond character, which are close to the experimentally determined B-N double bond length (1.400 Å) in aminoborane.[28]

The alternating strong and weak bonds evidenced also in the electron density at

the isocontour value of 0.20 a.u. (Figure 3.9) suggest an approximate "Kekulé-like" structure for these systems.

Similar to the results obtained for the boron-nitrogen helicenes, the energy results (Table 3.3) show the analogous gradual total energy contributions of unit structures with the increasing number of *N*. The values of energy changes are nearly constant, up to five digits, approximately -238.85 and -240.29 ± 0.01 Hartrees at the HF/6-31G(d) and the B3LYP/6-31G(d) levels, respectively.

By increasing the number of fused boron-nitrogen rings, extended helices BN[6]polymethylenylnaphthalenes, **9a** and NB[6]polymethylenylnaphthalenes, **9b** can be obtained (Figure 3.10).

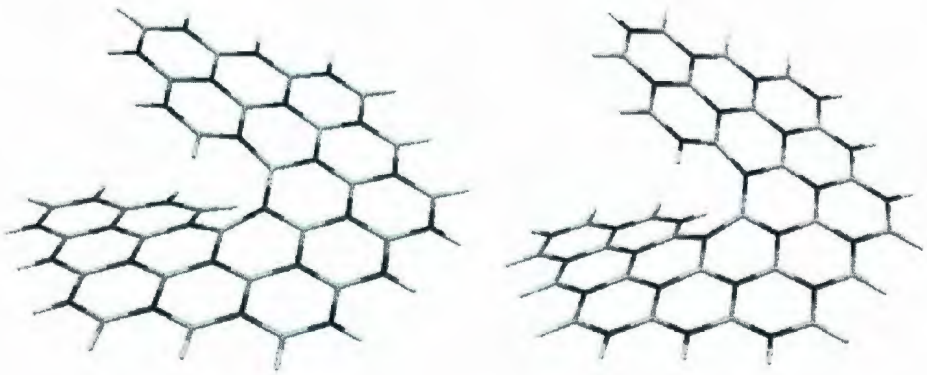

9a **9b**

Figure 3.10: The optimized geometries of extended BN and NB [6]polymethylenylnaphthalenes

Their optimized structures were obtained and it was found that they are station-

ary points corresponding to energy minima with real vibrational frequencies at the HF/6-31G(d) and the B3LYP/6-31G(d) level of theory.

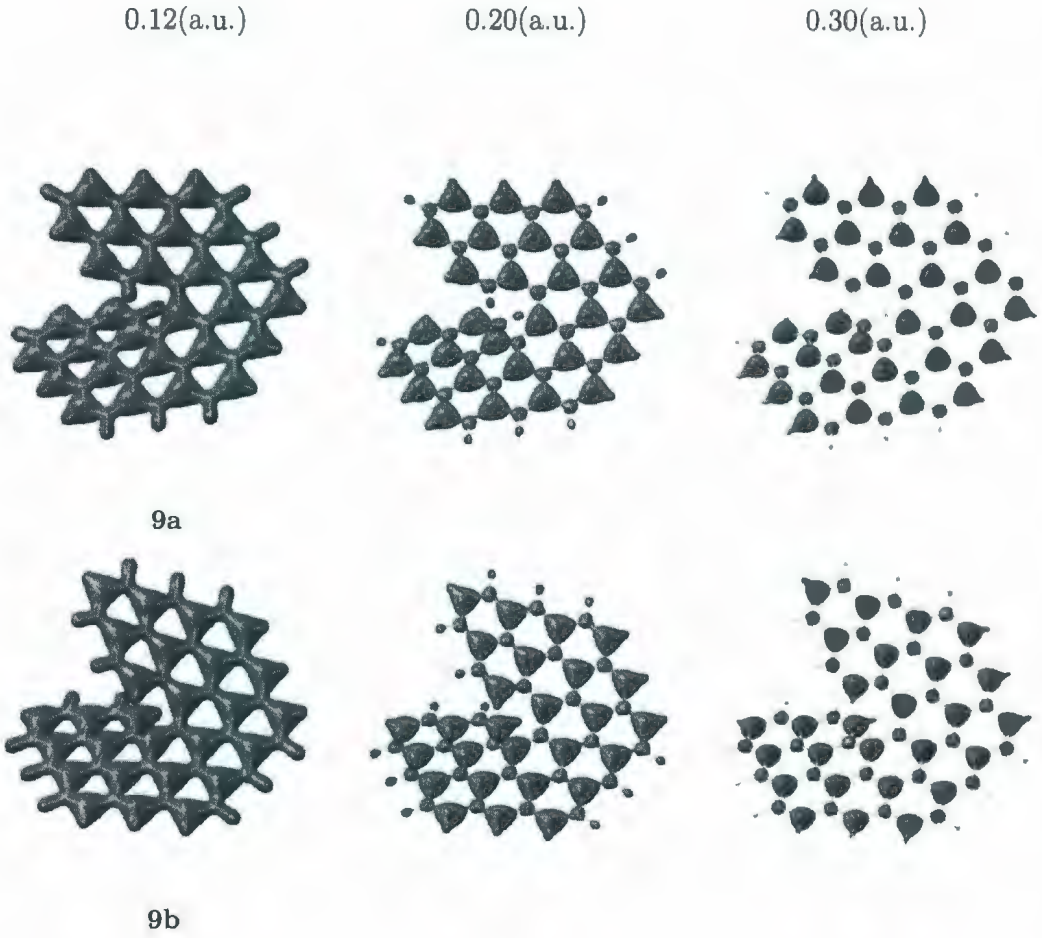

Figure 3.11: Electron density isocontours of single turn extended boron-nitrogen helices

The values of the six most characteristic B-N distances in the helices denoted by **a**, **b**, **c**, **d**, **e**, and **f** in Figure 3.7 range from 1.418 to 1.457 Å. From the electron

density shape analysis at the isocontour value of 0.20 a.u. (Figure 3.11), and from inspection of the optimized bond length values, it seems that the **a** type B-N bond is slightly stronger at the peripheries. This follows the general trend concerning the accumulation of electrons at the peripheries of the helices pointed out above.

3.4 Summary

Some novel boron-nitrogen analogues of angular helicenes, phenylenes and methylenylnaphthalenes were investigated. Attention was given to their geometries and energies as such molecules could provide useful information in the quest for novel boron-nitrogen based nanomaterials. The relative stability of the possible angular isomers was also discussed. These structures may serve as somewhat compressible, "spring-like" building blocks in supramolecular constructions.

The primary goal of this study was to investigate the structural viability of some boron-nitrogen systems, where the employed electron density analysis provided an alternative way for pointing out essential bonding features.

Bibliography

[1] I. Silaghi-Dumitrescu, I. Haiduc, and D. B Sowerby. *Inorg. Chem.*, 32(17):3755, 1993.

[2] G. Seifert, P.W. Fowler, D. Mitchell, D.and Porezag, and Th. Frauenheim. *Chem. Phys. Lett.*, 268:352, 1997.

[3] T. Oku, A. Nishiwaki, I. Narita, and M. Gonda. *Chem. Phys. Lett.*, 380:620, 2003.

[4] S. Xu, M. Zhang, Y. Zhao, B. Chen, J. Zhang, and C. Sun. *Chem. Phys. Lett.*, 418:297, 2006.

[5] M. S. Newman and D. Lednicer. *J. Am. Chem. Soc.*, 78:4765, 1956.

[6] S. Han, A. D. Bond, R. L. Disch, D. Holmes, J. M. Schulman, S.J. Teat, K. P. C. Vollhardt, and G. D. Whitener. *Angew. Chem. Int. Ed.*, 41:3223, 2002.

[7] T. J. Katz. *Angew. Chem. Int. Ed.*, 39:1921, 2000.

[8] K. E. S. Phillips, T. J. Katz, S. Jockusch, A. J. Lovinger, and N. J. Turro. *J. Am. Chem. Soc.*, 123:11899, 2001.

[9] J. M. Schulman and R. L. Disch. *J. Am. Chem. Soc.*, 118:8470, 1996.

[10] J. M. Schulman and R. L. Disch. *J. Phys. Chem. A*, 101:5596, 1997.

[11] J. M. Schulman and R. L. Disch. *J. Phys. Chem. A*, 103:6669, 1999.

[12] J. M. Schulman and R. L. Disch. *J. Phys. Chem. A*, 107:5223, 2003.

[13] L. Wang, P. L. Warburton, Z. Szekeres, P. Surjan, and P. G. Mezey. *J. Chem. Inf. Model.*, 45:850, 2005.

[14] A. Stock and E. Pohland. *Ber. Dtsch. Chem. Ges.*, 59:2215, 1926.

[15] A. W. Laubengayer, P. C. Moews Jr., and R. F. Porter. *J. Am. Chem. Soc.*, 83:1337, 1961.

[16] G. Mamantov and J. L. Margrave. *J. Inorg. Nucl. Chem.*, 20:348, 1961.

[17] M. A. Neiss and R. F. Porter. *J. Am. Chem. Soc.*, 94:1438, 1972.

[18] P. J. Fazen, E. E. Remsen, J.S. Beck, P.J. Carroll, A. R. McGhie, and L. G. Sneddon. *Chem. Mater.*, 7:1942, 1995.

[19] T. Kar, D. E. Elmore, and S. Scheiner. *J. Mol. Struct.(THEOCHEM)*, 392:65, 1997.

[20] N.C. Baird and M.A. Whitehead. *Can. J. Chem./Rev. Can. Chim.*, 45(18):2059, 1967.

[21] L. Turker. *J. Mol. Struct.(THEOCHEM)*, 640:63, 2003.

[22] A. K. Phukan, R. P. Kalagi, S. R. Gadre, and E. D. Jemmis. *Inorg. Chem.*, 43:5824, 2004.

[23] F. F. Xu, Y. Bando, R. Ma, D. Golberg, Y. Li, and M. Mitome. *J. Am. Chem. Soc.*, 125:8032, 2003.

[24] L. Wang and P. G. Mezey. *J. Phys. Chem. A*, 109:3241, 2005.

[25] A. D. Becke. *J. Chem. Phys.*, 98:5648, 1993.

[26] C. Lee, W. Yang, and R. G. Parr. *Phys. Rev. B*, 37:785, 1988.

[27] M. J. Frisch, G. W. Trucks, H. B. Schlegel, G. E. Scuseria, M. A. Robb, J. R. Cheeseman, Jr. Montgomery, J. A., T. Vreven, K. N. Kudin, J. C. Burant, J. M. Millam, S. S. Iyengar, J. Tomasi, V. Barone, B. Mennucci, M. Cossi, G. Scalmani, N. Rega, G. A. Petersson, H. Nakatsuji, M. Hada, M. Ehara, K. Toyota, R. Fukuda, J. Hasegawa, M. Ishida, T. Nakajima, Y. Honda, O. Kitao, H. Nakai, M. Klene, X. Li, J. E. Knox, H. P. Hratchian, J. B. Cross, V. Bakken, C. Adamo, J. Jaramillo, R. Gomperts, R. E. Stratmann, O. Yazyev, A. J. Austin, R. Cammi, C. Pomelli, J. W. Ochterski, P. Y. Ayala, K. Morokuma, G. A. Voth, P. Salvador, J. J. Dannenberg, V. G. Zakrzewski, S. Dapprich, A. D. Daniels, M. C. Strain,

O. Farkas, D. K. Malick, A. D. Rabuck, K. Raghavachari, J. B. Foresman, J. V. Ortiz, Q. Cui, A. G. Baboul, S. Clifford, J. Cioslowski, B. B. Stefanov, G. Liu, A. Liashenko, P. Piskorz, I. Komaromi, R. L. Martin, D. J. Fox, T. Keith, M. A. Al-Laham, C. Y. Peng, A. Nanayakkara, M. Challacombe, P. M. W. Gill, B. Johnson, W. Chen, M. W. Wong, C. Gonzalez, and J. A. Pople. *Gaussian 03, Revision C.02, Gaussian, Inc., Wallingford CT*, 2004.

[28] M. Sugie, H. Takeo, and C. Matsumura. *Chem. Phys. Lett.*, 64:573, 1979.

Chapter 4

Helices of boron-nitrogen hexagons and decagons. A theoretical study*

4.1 Introduction

Following the discovery of fullerene[1] and carbon nanotubes,[2] theoretical studies in the early 90's were already predicting the existence of their boron-nitrogen analogues.[3–5] The synthesis[6] of boron-nitride nanotubes (BNNTs) and later the experimental evidence[7, 8] for the first boron-nitrogen fullerene-like structures justified their structural characterization. These fully boron-nitrogen compounds proved to have high chemical and thermal stability.[9] Recently, the synthesis of novel boron-nitride helical conical nanotubes (BN HCNTs) having elastic properties was also reported.[10]

Due to their interesting electronic, thermal and mechanical properties, structures

*Adapted from: C. E. Szakacs and P. G. Mezey. *J. Phys. Chem. A*, 112(29):6783, 2008.

formed exclusively from boron and nitrogen could provide new options for novel materials with applications in nanotechnology. As a consequence, the theoretical study of the structure, stability, electronic and other properties of fully boron-nitrogen compounds has attracted considerable interest.[11–17]

The earlier chapter investigated the structure and stability of some boron-nitrogen analogues of more extended polyhelicenic hydrogenated helices, providing some additional information on extended boron-nitrogen compounds.

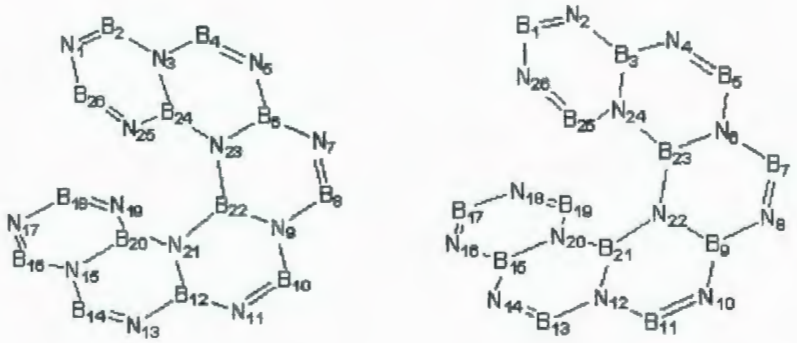

NB **BN**

Figure 4.1: The two types of nonhydrogenated boron-nitrogen angular helices NB and BN in case of six fused hexagons

It was observed that, in the case of boron-nitrogen analogues of helicenes, depending on the actual arrangements of the boron and nitrogen atoms in the terminal ring, an even number of N fused rings leads to the existence of stable angular isomers, shown in Figure 4.1. According to our notations, the two isomers are distinguished as follows: on the left hand side, the structures are called **NB** type helices, and the

right hand side structures are called **BN** type helices, respectively.

In the present chapter, further computational investigations are reported for a series of nonhydrogenated boron-nitrogen helices, formed by an even number N of fused boron-nitrogen hexagons and larger polygons.

The two types of initially assumed helical structures, **NB** and **BN**, convert to characteristically different equilibrium geometries, depicted in Figure 4.2 and Figure 4.3. The **NB** isomers have stable forms as helices **1-4** with 6, 8, 10, and 12 fused hexagons. The initially assumed helical **BN** isomers of hexagonal units, however, undergo ring opening at the terminal rings, leading to helices **5-8**, with 2, 4, 6, and 8 fused hexagons and 2 terminal decagons, respectively. Interchanging again the positions of B and N atoms in the latter **BN** type helices leads to additional isomers **9-12**.

The geometrical structures, bond lengths, and energies of all these isomeric structures were compared for a better understanding of their relative stability as such helices may become building blocks for more extended novel nanostructures.

4.2 Computational methodology

Geometry ptimization calculations were performed for a number of nonhydrogenated boron-nitrogen helices. The levels of theory used were HF and B3LYP with the 6-31G(d) basis set.[18, 19] In addition, single point energy calculations were also performed at MP2/6-31G(d) level of theory, using the HF/6-31G(d) optimized ge-

ometries. All these methods are implemented in the Gaussian 03 software package.[20] For verification of the energy minima for all optimized geometries, harmonic vibrational frequencies were computed at the same level of theory and zero point energy calculations have also been carried out. Electron density analysis was performed for some of the structures using DFT with the B3LYP functional and 6-31G(d) basis set for the purpose of obtaining additional information to help understand the bonding pattern in these systems.

4.3 Results and Discussions

4.3.1 Geometries and Bond Lengths

The optimized geometries of all the boron-nitrogen structures **1-12** are shown in Figure 4.2 and Figure 4.3. Note that all the optimized structures have helicoidal geometry except compound **5**, which is a partial helix, and compound **9**, which prefers a planar conformation.

All optimized structures are characterized to be minima by having real vibrational frequencies. The calculated lowest vibrational frequencies corresponding to primarily spring-like motions of the helical systems are shown in Table 4.1. The ease of such distortions is an indication of the potential application of these units in flexible nanostructures.

For the nonterminal rings of helices **1-4**, there are essentially four kinds of boron-

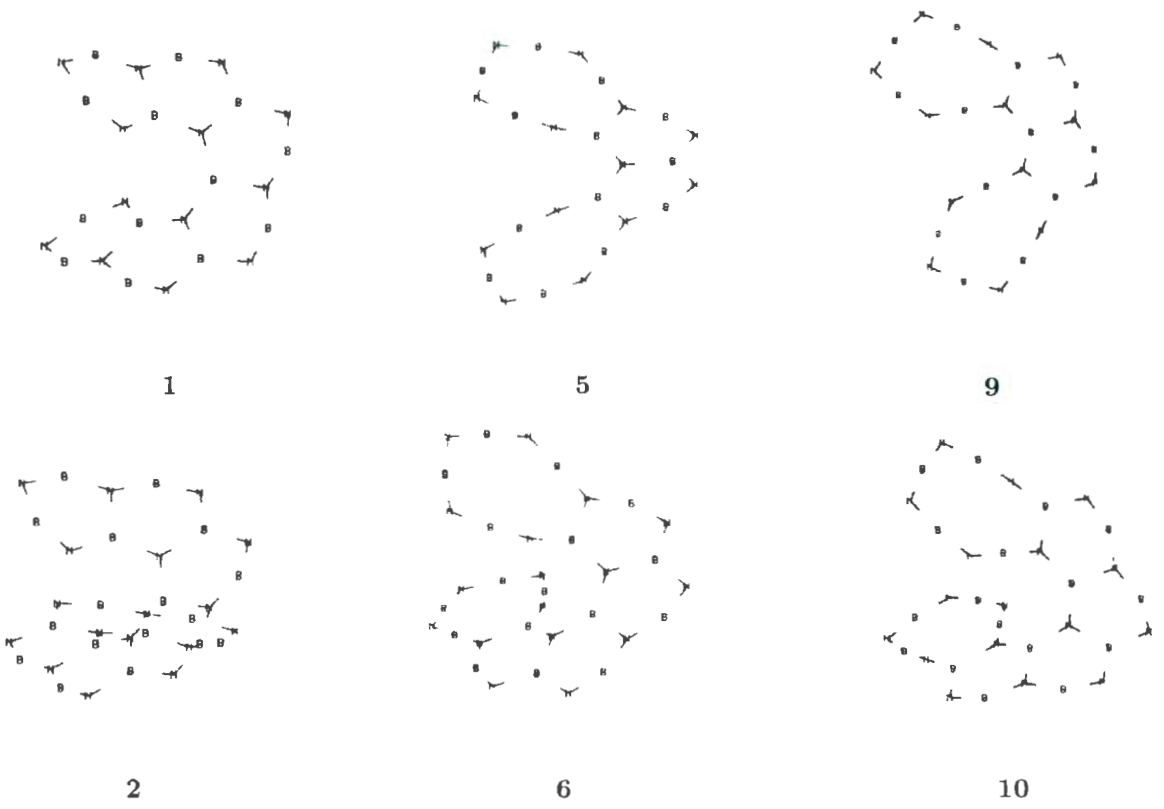

Figure 4.2: The optimized geometries at B3LYP/6-31G(d) level of theory

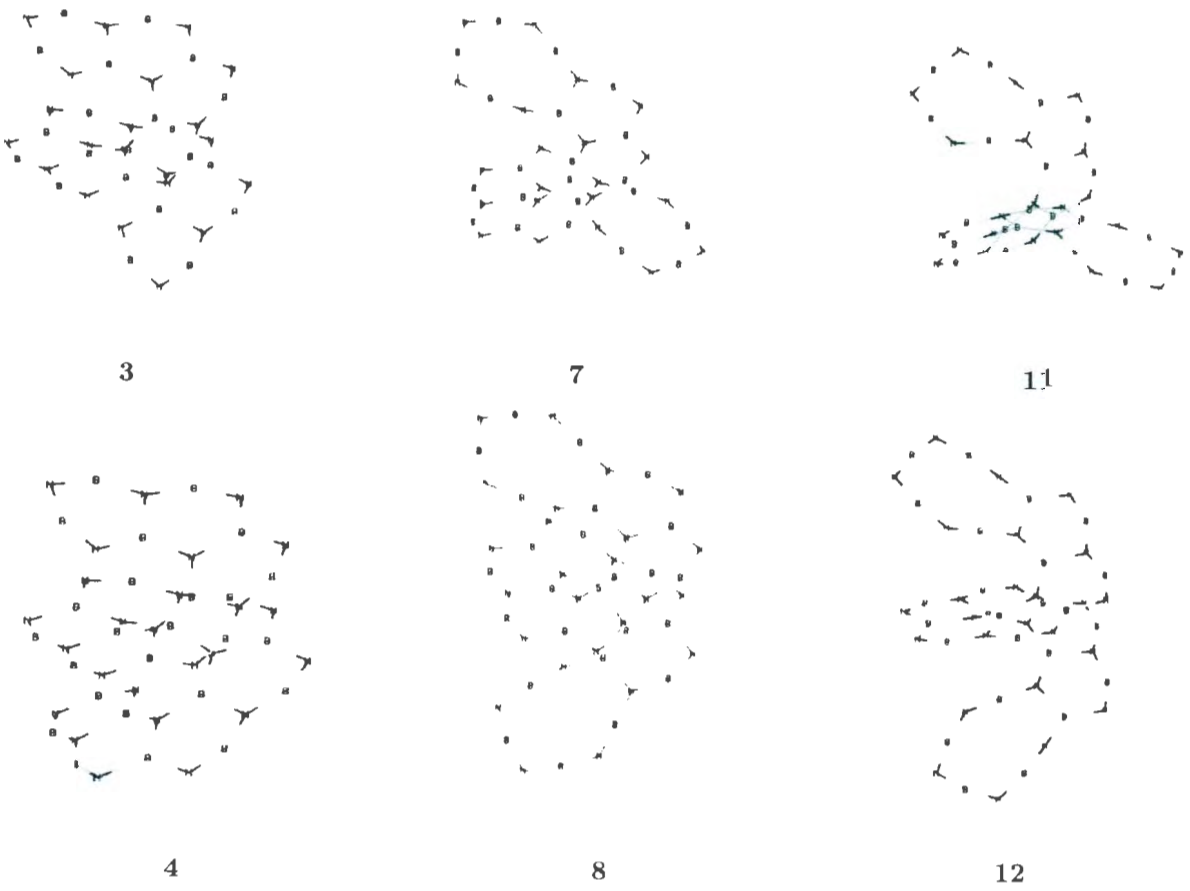

Figure 4.3: The optimized geometries at B3LYP/6-31G(d) level of theory

Table 4.1: The lowest wavenumbers (cm^{-1}) of the studied boron-nitrogen helices **1-12**. (Calculated values at HF/6-31G(d) shown in the second column, followed by those at B3LYP/6-31G(d) in the third column)

1	40.60	37.54
2	29.51	18.35
3	34.92	31.93
4	33.01	31.47
5	19.80	9.66
6	16.55	15.30
7	21.15	18.03
8	25.31	22.69
9	13.00	15.06
10	17.00	17.12
11	17.54	17.06
12	18.50	16.63

nitrogen bond lengths denoted *j*, *k*, *l*, and *m* (Figure 4.4). Whereas the two bond lengths *j* and *k* tend to be larger, the bond length *m* is shorter, indicating bonds that are stronger at the peripheries of the helices. The two end-rings show major deviations when compared to the inner units of the helices.

The final optimized structures **5-12** show a ring opening at the two original ter-

minal hexagons, leading to the formation of boron-nitrogen decagons at both ends.

	1 (N=4)*	**2** (N=6)	**3** (N=8)	**4** (N=10)
$j =$	1.449-1.452	1.444-1.468	1.442-1.461	1.446-1.462
$k =$	1.552-1.664	1.550-1.661	1.550-1.652	1.549-1.649
$l =$	1.376-1.444	1.372-1.447	1.376-1.444	1.374-1.445
$m =$	1.279-1.282	1.279-1.284	1.278-1.283	1.277-1.286

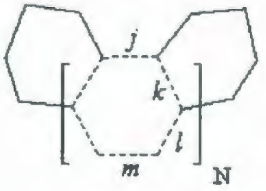

Figure 4.4: Bond lengths (in Ångströms) at B3LYP/6-31G(d) level of theory for helices **1**, **2**, **3**, and **4**.

*The N from the schematic representation of the structures represents the number of inner hexagons. This is valid also for Figure 4.5 and Figure 4.6.

This ring opening tendency may be partly due to the preference of boron atoms to form colinear bonds when placed between two nitrogen atoms. The four bond types denoted by *j*, *k*, *l*, and *m*, observed in helices **1-4** are characteristic for the inner hexagons of the helices **5-12** as well. However, for the terminal rings of the structures **5-12**, nine types of boron-nitrogen bond lengths can be observed, denoted

	5 (N=2)	**6** (N=4)	**7** (N=6)	**8** (N=8)
$a =$	1.363	1.362	1.365	1.366
$b =$	1.297	1.297	1.294	1.294
$c =$	1.338	1.337	1.338	1.338
$d =$	1.318	1.319	1.318	1.318
$e =$	1.349	1.348	1.347	1.346
$f =$	1.319	1.320	1.321	1.323
$g =$	1.358	1.357	1.353	1.352
$h =$	1.289	1.290	1.293	1.294
$i =$	1.372	1.380	1.378	1.378
$j =$	1.465	1.451-1.457	1.445-1.459	1.446-1.461
$k =$	1.568-1.600	1.554-1.591	1.551-1.592	1.551-1.587
$l =$	1.384-1.445	1.375-1.448	1.374-1.452	1.377-1.448
$m =$	1.278	1.277-1.282	1.279-1.284	1.278-1.285

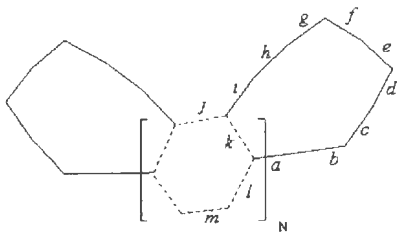

Figure 4.5: Bond lengths (in Ångströms) at B3LYP/6-31G(d) level of theory for helices **5**, **6**, **7**, and **8**.

	9 (N=2)	**10** (N=4)	**11** (N=6)	**12** (N=8)
$a =$	1.375	1.374	1.373	1.373
$b =$	1.298	1.300	1.300	1.300
$c =$	1.336	1.338	1.337	1.337
$d =$	1.319	1.318	1.319	1.319
$e =$	1.349	1.349	1.349	1.349
$f =$	1.321	1.321	1.321	1.321
$g =$	1.358	1.358	1.359	1.359
$h =$	1.290	1.290	1.290	1.290
$i =$	1.375	1.375	1.376	1.376
$j =$	1.448	1.448-1.452	1.449-1.455	1.448-1.455
$k =$	1.521-1.621	1.529-1.614	1.529-1.614	1.532-1.616
$l =$	1.386-1.439	1.382-1.441	1.380-1.439	1.380-1.439
$m =$	1.279	1.279-1.281	1.279-1.281	1.279-1.281

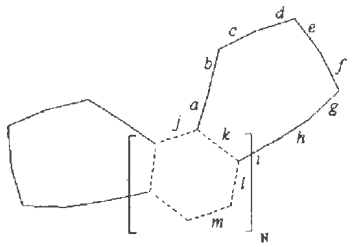

Figure 4.6: Bond lengths (in Ångströms) at B3LYP/6-31G(d) level of theory for helices **9, 10, 11,** and **12**.

by *a*, *b*, *c*, *d*, *e*, *f*, *g*, *h*, and *i* (Figure 4.5 and 4.6). The corresponding bond lengths in the two decagons have the same values at both ends in all the structures due to symmetry reasons. Upon examining the bond lengths in the terminal polygon in each case (**5-12**), one can conclude that these bonds are consistently strong, much stronger than bond types *k* and *j*.

4.3.2 Electron density analysis

Electron density calculations were performed for the helices **2, 6,** and **10**, as well as for the largest optimized structures **4, 8,** and **12**, using density functional theory. The detailed electron density shape analysis of these molecules (Figure 4.7) provide a justification and are in strong agreement with the bond length considerations.

The shape analysis shows a higher level of electron density distribution in the terminal rings (being decagons in helices **6, 8, 10,** and **12**, and hexagons in helices **2** and **4**) as well as along the peripheries for all the helices where the alternating pattern due to the alternation of boron and nitrogen atoms is well manifested.

This electron density enrichment in the terminal and peripheral regions is probably due to the tendency of even partial systems for allowing electron repulsion to enhance arrangements with accumulations of electrons far apart, resulting in stronger bonds in the terminal rings and peripheries, respectively. Looking at the nonterminal rings, especially where both the boron and the nitrogen atoms are trivalent, there

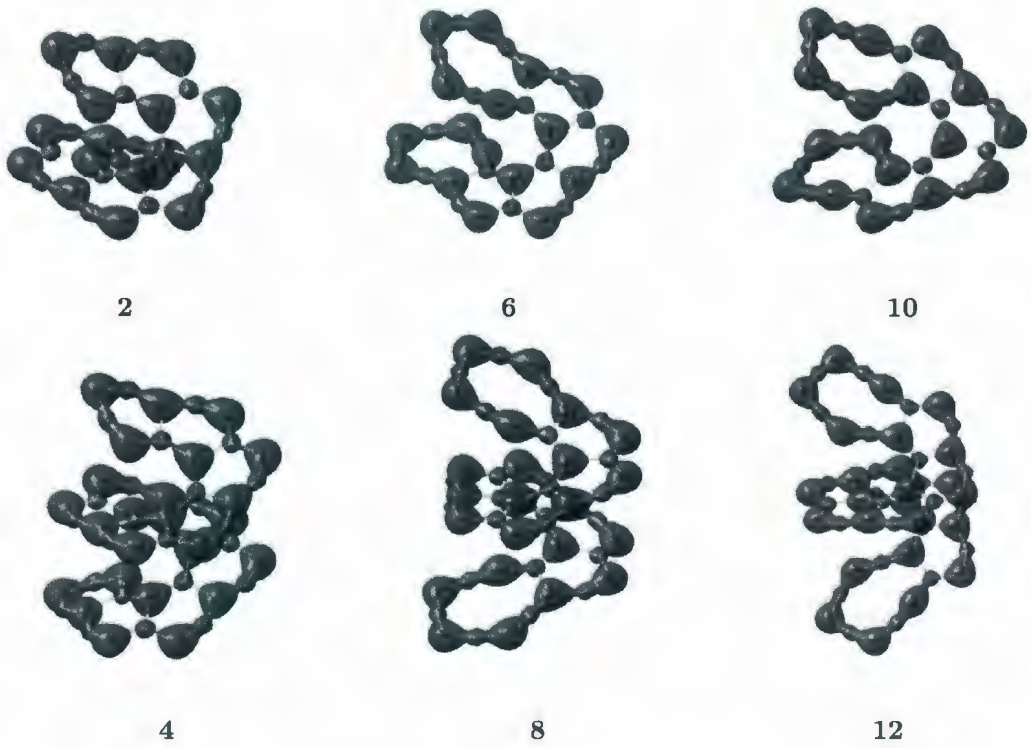

Figure 4.7: Electron density isocontours of helices **2** (with eight fused hexagons), **6** and **10** (with four fused hexagons and two terminal decagons) and helices **4** (with twelve fused hexagons), **8** and **12** (with eight fused hexagons and two terminal decagons)at 0.20 a.u.

is a depletion in the electron density (shown as discontinuity in the actual electron density contours at 0.20 a.u.). This fact is also manifested in longer bond lengths in the inner hexagons.

4.3.3 Energies

In all three types of helices, as the number of fused rings increases, a nearly exactly linear decrease in the total energy is observed (Table 4.2). The helices **5-8** are energetically more stable than the helices **1-4**. The ring opening and formation of decagons at the two terminal rings seem to enhance their relative stability. The difference in the relative energy values between the two types of helices ranges between 88.4 and 91.7 kcal/mol at the HF/6-31G(d) level, and between 75.0 and 78.9 kcal/mol at B3LYP/6-31G(d) level. The relative energy differences calculated at the MP2/6-31G(d)//HF/6-31G(d) are lower in value, but follow a similar trend.

The inclusion of ZPVE correction in estimating the relative energies does not modify the ordering and the considerable differences between isomers (Table 4.2).

When comparing the **5-8** type helices to their **9-12** counterparts, it should be noted that structure **9** has a planar conformation, and contrary to the overall trend, it is lower in energy than the partial helix **5** by approximately 1.3 kcal/mol at the HF/6-31G(d) level and by approximately 1.5 kcal/mol at the B3LYP/6-31G(d) level of theory (Table 4.2). However, the fully helicoidal structures **10, 11,** and **12** are higher in energy than the helices **6, 7,** and **8**, by approximately 1.7, 5.5, and 7.2 kcal/mol at the HF/6-31G(d) level of theory and by 0.8, 3.3, and 4.6 kcal/mol at the B3LYP/6-31G(d) level of theory, respectively. The relative energy differences calculated at the MP2/6-31G(d)//HF/6-31G(d) follow the same trend.

Table 4.2: Calculated total energies (E, in Hartree), relative energies** (ΔE, in kcal/mol), sum of total and zero-point vibrational energies (E + ZPVE, in Hartree), relative energies including ZPVE (ΔE', in kcal/mol), and single point energies (E_{sp}, in Hartree) for boron-nitrogen helices **1-12**

Molecule	HF/6-31G(d)				B3LYP/6-31G(d)				MP2/6-31G(d)	
	T	ΔE	E + ZPVE	ΔE'	E	ΔE	E + ZPVE	ΔE'	E_{sp}	ΔE
1	-1029.4354	88.4	-1029.3026	89.4	-1035.4972	77.3	-1035.3734	77.7	-1032.4391	58.4
2	-1346.2350	86.3	-1346.0600	87.3	-1354.1588	75.0	-1353.9958	75.4	-1350.1728	54.3
3	-1663.0285	90.0	-1662.8113	91.0	-1672.8160	77.5	-1672.6135	77.9	-1667.9026	58.2
4	-1979.8189	91.7	-1979.5597	92.6	-1991.4709	78.9	-1991.2292	79.2	-1985.6301	60.1
5	-1029.5763	0.0	-1029.4450	0.0	-1035.6203	0.0	-1035.4973	0.0	-1032.5321	0.0
6	-1346.3726	0.0	-1346.1992	0.0	-1354.2783	0.0	-1354.1159	0.0	-1350.2594	0.0
7	-1663.1719	0.0	-1662.9562	0.0	-1672.9395	0.0	-1672.7377	0.0	-1667.9955	0.0
8	-1979.9651	0.0	-1979.7073	0.0	-1991.5966	0.0	-1991.3554	0.0	-1985.7259	0.0
9	-1029.5784	-1.3	-1029.4471	-1.3	-1035.6228	-1.6	-1035.4997	-1.5	-1032.5348	-1.7
10	-1346.3698	1.7	-1346.1963	1.8	-1354.2775	0.5	-1354.1150	0.5	-1350.2561	2.1
11	-1663.1632	5.5	-1662.9477	5.4	-1672.9343	3.3	-1672.7326	3.2	-1667.9850	6.6
12	-1979.9536	7.2	-1979.6961	7.0	-1991.5893	4.6	-1991.3485	4.4	-1985.7128	8.3

All relative energy values are calculated in comparison to the set of helices **5-8, for which a relative energy of zero is assigned.

4.4 Summary

The initially assumed helical **BN** isomers of hexagonal units undergo a ring opening in the terminal rings due to the boron atom's preference for linearity. Comparing the energy values of the fully optimized ground states, it can be concluded that the ring opening stabilizes the helices containing terminal decagon rings. Again, by alternating the boron and nitrogen atoms in these helices, new isomers are obtained. In the present study, attention was given to the relative stability, geometry, bonding pattern, and energies of these isomeric helices as such molecules could provide useful information in the quest for novel materials based fully on boron and nitrogen. These structures are rather flexible and behave like "nano-springs", suggesting new possibilities, and may become models towards the synthesis of new, helical boron-nitrides.

Bibliography

[1] H. W. Kroto, J. R. Heath, S.C. O'Brien, R. F. Curl, and R. E. Smalley. *Nature*, 318:162, 1985.

[2] S Iijima. *Nature*, 354:56, 1991.

[3] I. Silaghi-Dumitrescu, I. Haiduc, and D. B Sowerby. *Inorg. Chem.*, 32(17):3755, 1993.

[4] X. Xia, D. A. Jelski, J. R. Bowser, and T. F. George. *J. Am. Chem. Soc.*, 114 (16):6493, 1992.

[5] A. Rubio, J. L. Corkill, and M. L. Cohen. *Phys. Rev. B*, 49:5081, 1994.

[6] N. G. Chopra, Luyken R. J., Cherrey K., V. H. Crespi, M. L. Cohen, Louie S. G., and A. Zettl. *Science*, 269:966, 1995.

[7] O. Stephan, Y. Bando, A. Loiseau, F. Willaime, N. Shramchenko, T. Tamiya, and T. Sato. *Appl. Phys. A*, 67:107, 1998.

[8] D. Golberg, Y. Bando, O. Stephan, and K. Kurashima. *Appl. Phys. Lett.*, 73:2441, 1998.

[9] W. Q. Han, W. Mickelson, J. Cumings, and A. Zettl. *Appl. Phys. Lett.*, 81:1110, 2002.

[10] F. F. Xu, Y. Bando, R. Ma, D. Golberg, Y. Li, and M. Mitome. *J. Am. Chem. Soc.*, 125:8032, 2003.

[11] G. Seifert, P.W. Fowler, D. Mitchell, D.and Porezag, and Th. Frauenheim. *Chem. Phys. Lett.*, 268:352, 1997.

[12] J. Kongsted, A. Osted, L. Jensen, P.-O. Astrand, and K. V. Mikkelsen. *J. Phys. Chem. B*, 105:10243, 2001.

[13] D. L. Strout. *Chem. Phys. Lett.*, 383:95, 2004.

[14] I. Silaghi-Dumitrescu, F. Lara-Ochoa, P. Bishof, and I. Haiduc. *J. Mol. Struct.(THEOCHEM)*, 367:47, 1996.

[15] H. S. Wu, X. Y. Cui, and X. H. Xu. *J. Mol. Struct.(THEOCHEM)*, 717:107, 2005.

[16] S. Xu, M. Zhang, Y. Zhao, B. Chen, J. Zhang, and C. Sun. *Chem. Phys. Lett.*, 418:297, 2006.

[17] R. J. C. Batista, M. S. C. Mazzoni, and Chacham H. *Chem. Phys. Lett.*, 421:246, 2006.

[18] A. D. Becke. *J. Chem. Phys.*, 98:5648, 1993.

[19] C. Lee, W. Yang, and R. G. Parr. *Phys. Rev. B*, 37:785, 1988.

[20] M. J. Frisch, G. W. Trucks, H. B. Schlegel, G. E. Scuseria, M. A. Robb, J. R. Cheeseman, Jr. Montgomery, J. A., T. Vreven, K. N. Kudin, J. C. Burant, J. M. Millam, S. S. Iyengar, J. Tomasi, V. Barone, B. Mennucci, M. Cossi, G. Scalmani, N. Rega, G. A. Petersson, H. Nakatsuji, M. Hada, M. Ehara, K. Toyota, R. Fukuda, J. Hasegawa, M. Ishida, T. Nakajima, Y. Honda, O. Kitao, H. Nakai, M. Klene, X. Li, J. E. Knox, H. P. Hratchian, J. B. Cross, V. Bakken, C. Adamo, J. Jaramillo, R. Gomperts, R. E. Stratmann, O. Yazyev, A. J. Austin, R. Cammi, C. Pomelli, J. W. Ochterski, P. Y. Ayala, K. Morokuma, G. A. Voth, P. Salvador, J. J. Dannenberg, V. G. Zakrzewski, S. Dapprich, A. D. Daniels, M. C. Strain, O. Farkas, D. K. Malick, A. D. Rabuck, K. Raghavachari, J. B. Foresman, J. V. Ortiz, Q. Cui, A. G. Baboul, S. Clifford, J. Cioslowski, B. B. Stefanov, G. Liu, A. Liashenko, P. Piskorz, I. Komaromi, R. L. Martin, D. J. Fox, T. Keith, M. A. Al-Laham, C. Y. Peng, A. Nanayakkara, M. Challacombe, P. M. W. Gill, B. Johnson, W. Chen, M. W. Wong, C. Gonzalez, and J. A. Pople. *Gaussian 03, Revision C.02, Gaussian, Inc., Wallingford CT*, 2004.

Chapter 5

Laterally extended spiral graphite analogue boron-nitrogen helices*

5.1 Introduction

Borazine based polymers are being considered as precursors for the synthesis of boron-nitride ceramics.[1, 2] An earlier theoretical study[3] investigated molecules containing up to three fused borazine rings, predicting the possibility of boron-nitrogen polymers containing larger numbers of six-membered rings. Further studies[4, 5] reported also on the stability of "cycled-fused-borazines", belt-like structures, analogues of the carbon based cyclacenes, and on the boron-nitrogen analogues of acenes, structures comprised of linearly fused borazine rings.

The investigation in previous chapters focused on the structure, energy, and rel-

*Adapted from: C. E. Szakacs and P. G. Mezey. *J. Phys. Chem. A*, 113(17):5157, **2009**

ative stability of hydrogenated boron-nitrogen analogues of angular fused-ring structures, like helicenes, phenylenes, and single turn polymethylenylnaphthalenes and nonhydrogenated boron-nitrogen analogues of helicenes, respectively.

In this chapter, computational investigations on a series of laterally extended boron-nitrogen helices are reported. The carbon analogue was studied recently,[6] at HF/6-31G(d) level of theory, being considered a "model toward helical graphites". The single-turn boron-nitrogen analogue of polymethylenylnaphthalene comprised of six fused units was briefly discussed in Chapter 3. Although derivable from one-another by interchanging nitrogen and boron atoms, they are very similar but not isomeric structures. For isomerism, an even number of heavy atoms in the fused borazine rings or hexagonal type units is required, generated by the alternation of the positions of the boron and nitrogen atoms. In the case of the boron-nitrogen analogues of polymethylenylnapthalenes, which are comprised of an odd number of fused rings, this is not generally fulfilled and further discussion on this matter will follow in the next sections of the present chapter.

These structures are likely to serve as building blocks in the synthesis of novel spring-like helical boron-nitride compounds with applications in nanotechnology, especially if flexible interconnecting building units between geometrically distant functional units are needed.

5.2 Computational methodology

Geometry optimization of all the boron-nitrogen helices were performed at the Hartree-Fock and DFT level of theory using the B3LYP hybrid functional[7, 8] with the use of the 6-31G(d,p) basis set as implemented in the Gaussian 03 software package.[9] Vibrational frequencies were computed by determining the second derivatives of the energy for all optimized geometries at the same levels of theory in order to verify the energy minima.

5.3 Results and Discussions

5.3.1 Boron-nitrogen analogues of [*N*]polymethylenylnaphthalene

Geometries of the optimized structures of the boron-nitrogen analogues of [N]polymethylenylnaphthalene (N = 6, 8, and 12) are depicted in Figure 5.1, Figure 5.2, and Figure 5.3. An interesting aspect of these helices is that the alternation of the positions of the boron and the nitrogen atoms leads to very similar helical conformations. Even though the number of existing bonds and the number of atoms in both structures are the same, the total number of heavy atoms is odd, hence one of the helices has an extra nitrogen atom and the other has an extra boron atom.

From now on we will refer to these structures as the $N_xB_yH_z$ helices (**1, 3,** and **5**) and the $B_xN_yH_z$ helices (**2, 4,** and **6**), where the $y = x - 1$ relation is valid generally. Investigations on all the optimized helices **1-6** confirmed the existence of energy

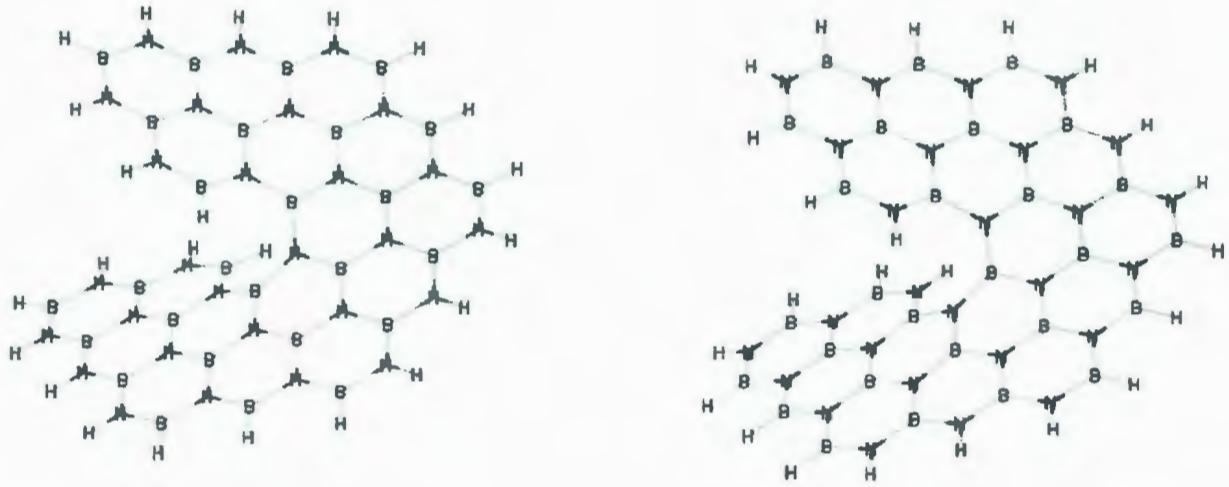

1,($N_{28}B_{27}H_{23}$) **2**, ($B_{28}N_{27}H_{23}$)

Figure 5.1: The optimized geometries of boron-nitrogen helices **1-2**

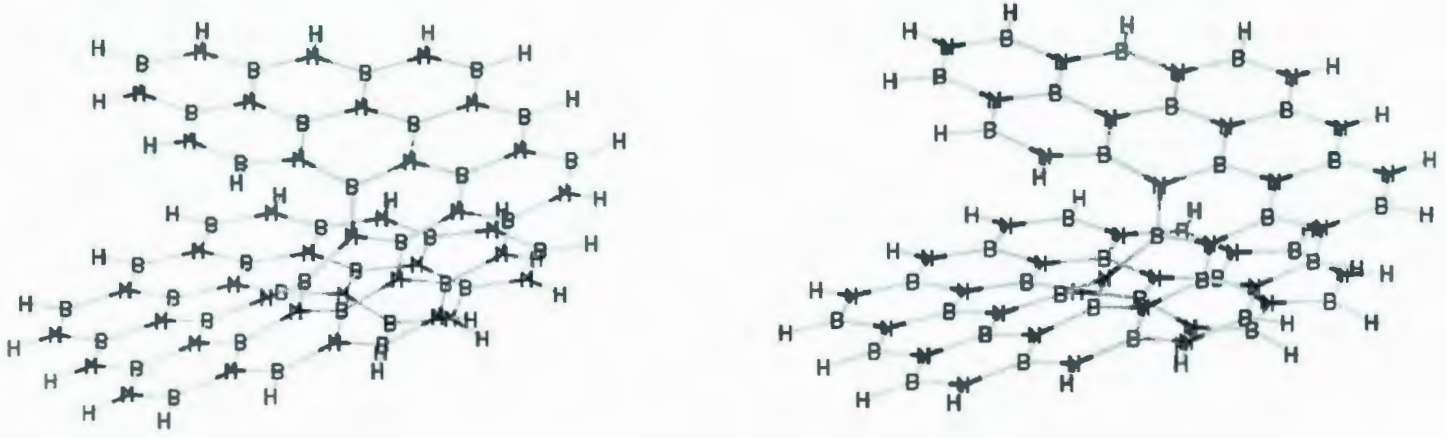

3, $(N_{37}B_{36}H_{29})$ **4**, $(B_{37}N_{36}H_{29})$

Figure 5.2: The optimized geometries of boron-nitrogen helices **3-4**

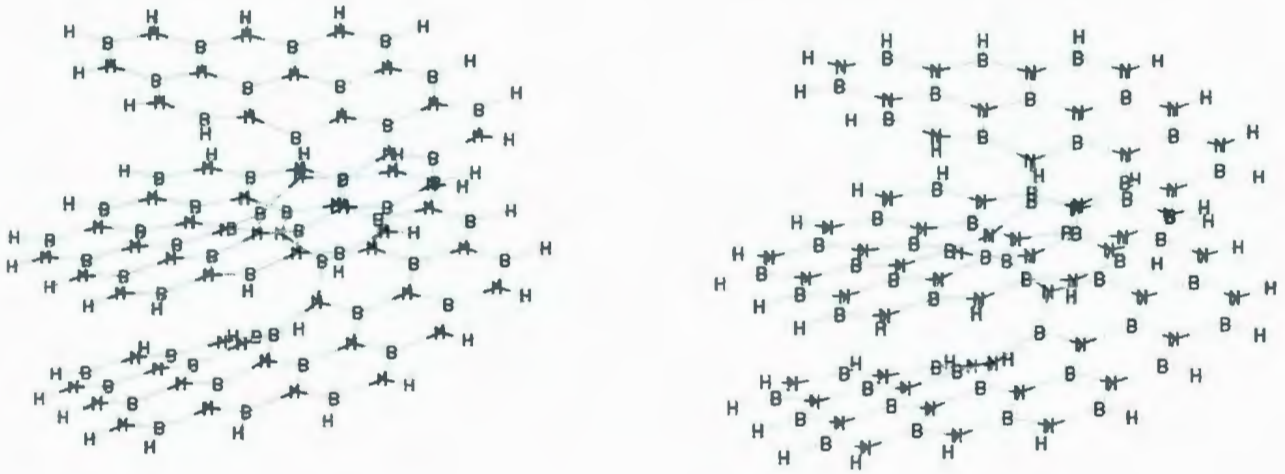

5, $(N_{55}B_{54}H_{41})$ **6**, $(B_{55}N_{54}H_{41})$

Figure 5.3: The optimized geometries of boron-nitrogen helices **5-6**

minima by having real vibrational frequencies at both levels of theory. The lowest vibrational frequencies correspond to spring-like motions, observed also in the helical systems studied in the earlier chapters, a potentially useful aspect in nanotechnology.

helix	bond type *a*	bond type *g*
1	1.418 -1.419 (1.422 - 1.423)	1.454 - 1.455 (1.458 - 1.459)
2	1.418 -1.419 (1.422)	1.456 - 1.457 (1.461 - 1.463)
3	1.418 -1.419 (1.422 - 1.423)	1.453 - 1.457 (1.457 - 1.461)
4	1.418 -1.419 (1.421 - 1.423)	1.452 - 1.460 (1.457 - 1.465)
5	1.418 -1.419 (1.423 - 1.424)	1.455 - 1.458 (1.459 - 1.462)
6	1.418 -1.420 (1.422 - 1.424)	1.453 - 1.460 (1.456 - 1.465)

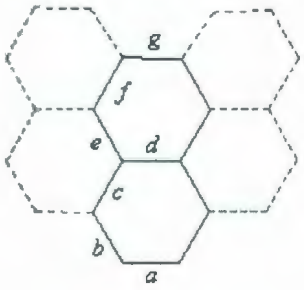

Figure 5.4: Bond lengths (in Ångströms) at HF and DFT (in parenthesis) level of theory for peripheral bond type *a* and inside loop bond type *g* in the optimized boron-nitrogen helices **1-6**.

Marked with *a, b, c, d, e, f,* and *g* in Figure 5.4 are the calculated bond lengths of the boron-nitrogen helices. The areas at the peripheries of the helices characterized by bond type *a*, resemble partial aminoborane fragments.

Table 5.1: Calculated energies (in Hartree) of the optimized boron-nitrogen helices **1-6**

Molecule	Levels of theory	
	HF/6-31G(d,p)	B3LYP/6-31G(d,p)
1, $N_{28}B_{27}H_{23}$	-2207.6926	-2220.9482
2, $B_{28}N_{27}H_{23}$	-2177.8993	-2191.0206
3, $N_{37}B_{36}H_{29}$	-2924.4829	-2942.0206
4, $B_{37}N_{36}H_{29}$	-2894.6996	-2912.0923
5, $N_{55}B_{54}H_{41}$	-4358.0604	-4384.1620
6, $B_{55}N_{54}H_{41}$	-4328.2679	-4354.2343

In these cases, bond type *a* has a pronounced double-bond character (1.418-1.419 Å), close to the value in the real aminoborane[10](1.400 Å). Bond type *g* connects trivalent boron and nitrogen atoms in the inner part of the helices, is weaker in strength, and can have a determining factor in the curvature of the helices. As seen in Figure 5.4, bond type *g* increases in length slightly going from the simple helices **1** and **2** to the larger helices **5** and **6**, whereas bond type *a* remains almost constant throughout the series at both levels of theory.

The values of the remaining bond types *b*, *c*, *d*, *e*, and *f* are between 1.429-1.452 Å at the HF and 1.433-1.457 Å at the density functional levels of theory. The bonding pattern appears to be stable and equilibrated, in agreement with the results of electron density calculations, shown in density isocontours at 0.20 a.u. seen in Figure 5.5, showing the pattern of strong and weak bonds.

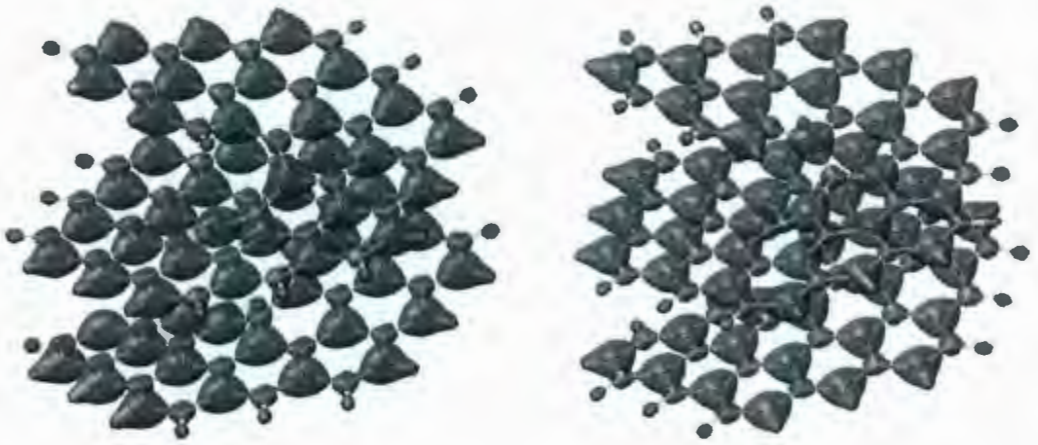

5 **6**

Figure 5.5: Electron density isocountours of helices **5** and **6** at 0.20 a.u.

From an energetic point of view, the difference between the two types of extended helices is around 30 Hartree, which is consistent with the energy difference between a boron and a nitrogen atom.

5.3.2 Laterally extended boron-nitrogen helical isomers

Taking into consideration the number of fused hexagonal units in the case of boron-nitrogen analogues of polymethylenylnaphthalenes presented earlier, one finds that they are generally comprised of an odd number of rings, 17 in case of helices **1** and **2**, 23 in case of helices **3** and **4**, and 35 fused rings in case of helices **5** and **6**. However if one more ring is attached to one of the ends of helix **1**, ($N_{28}B_{27}H_{23}$) or helix **2**,($B_{28}N_{27}H_{23}$), one gets two helical isomers, **7** and **8**. These are comprised of an even number (18) of fused rings having the formula $N_{29}B_{29}H_{24}$ and $B_{29}N_{29}H_{24}$ (Figure 5.6).

The ground state energies for the two isomers are shown in Table 5.2, the relative difference between the two helices being 3.2 kcal/mol at the Hartree-Fock and 3.8 kcal/mol at the density functional theory.

Table 5.2: Total energies (in Hartree) of laterally extended boron-nitrogen helical isomers

Molecule	Level/Basis set	
	HF/6-31G(d)	B3LYP/6-31G(d)
7, $N_{29}B_{29}H_{24}$	-2312.2596 (3.2)	-2326.1611(3.8)
8, $B_{29}N_{29}H_{24}$	-2312.2648 (0.0)	-2326.1672(0.0)

*The values in parenthesis show the energy in kcal/mol of the isomer **7**, relative to isomer **8**.

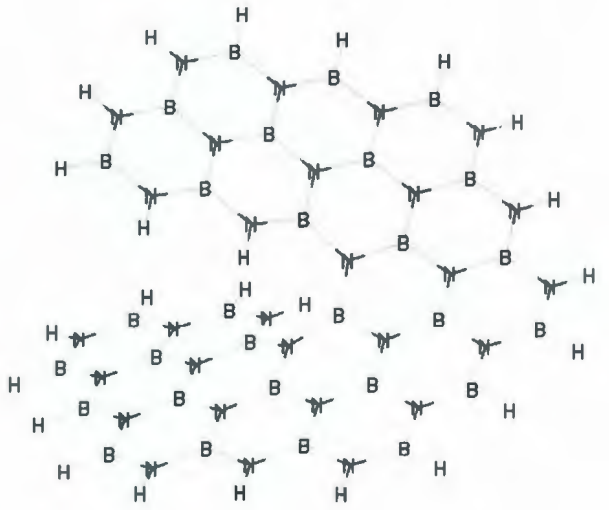

7

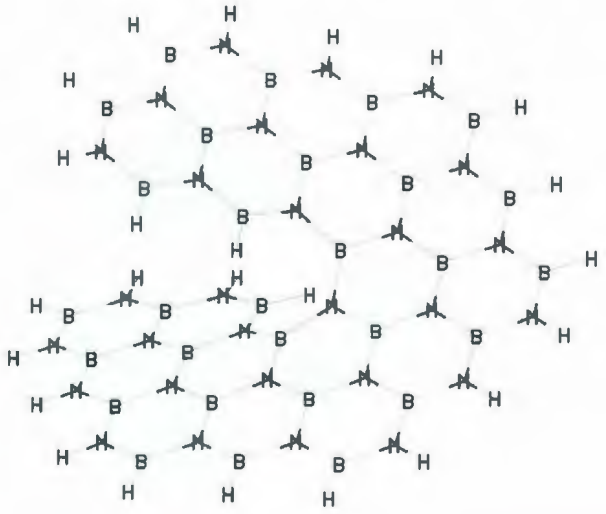

8

Figure 5.6: Helical isomers in case of an even number (18) of fused rings

Although full optimizations were performed only for helices containing 18 fused hexagonal units, it is clear that fusing one more hexagonal unit to the helices **3**, **5** or **4**, **6** leads to the same kind of isomerism.

5.4 Summary

The electronic structure of novel laterally extended boron-nitrogen helices was investigated. These structures may serve as potential models for spring-like nanostructures, where electronic and stability properties can be influenced by outside interactions with the electron-rich N atoms, and alternatively, by the electron-poor B atoms. By alternating the positions of the boron and nitrogen atoms, two very similar structures are possible, the $N_xB_yH_z$ helix (**1**, **3**, and **5**) and $B_xN_yH_z$ helix (**2**, **4**, and **6**). The same alternation of the boron and the nitrogen atoms in the laterally extended helices containing even number of fused hexagonal units leads to angular isomers. Such isomerism could have importance by providing alternatives of having the "right atom in the right place" in nanosprings, where strong or weak links to various locations along the spring are needed.

Bibliography

[1] R. T. Paine and C. K. Narula. *Chem. Rev.*, 90:73, 1990.

[2] P. J. Fazen, E. E. Remsen, J.S. Beck, P.J. Carroll, A. R. McGhie, and L. G. Sneddon. *Chem. Mater.*, 7:1942, 1995.

[3] N.C. Baird and M.A. Whitehead. *Can. J. Chem./Rev. Can. Chim.*, 45(18):2059, 1967.

[4] L. Turker. *J. Mol. Struct.(THEOCHEM)*, 640:63, 2003.

[5] A. K. Phukan, R. P. Kalagi, S. R. Gadre, and E. D. Jemmis. *Inorg. Chem.*, 43:5824, 2004.

[6] L. Wang, P. L. Warburton, Z. Szekeres, P. Surjan, and P. G. Mezey. *J. Chem. Inf. Model.*, 45:850, 2005.

[7] A. D. Becke. *J. Chem. Phys.*, 98:5648, 1993.

[8] C. Lee, W. Yang, and R. G. Parr. *Phys. Rev. B*, 37:785, 1988.

[9] M. J. Frisch, G. W. Trucks, H. B. Schlegel, G. E. Scuseria, M. A. Robb, J. R. Cheeseman, Jr. Montgomery, J. A., T. Vreven, K. N. Kudin, J. C. Burant, J. M. Millam, S. S. Iyengar, J. Tomasi, V. Barone, B. Mennucci, M. Cossi, G. Scalmani, N. Rega, G. A. Petersson, H. Nakatsuji, M. Hada, M. Ehara, K. Toyota, R. Fukuda, J. Hasegawa, M. Ishida, T. Nakajima, Y. Honda, O. Kitao, H. Nakai, M. Klene, X. Li, J. E. Knox, H. P. Hratchian, J. B. Cross, V. Bakken, C. Adamo, J. Jaramillo, R. Gomperts, R. E. Stratmann, O. Yazyev, A. J. Austin, R. Cammi, C. Pomelli, J. W. Ochterski, P. Y. Ayala, K. Morokuma, G. A. Voth, P. Salvador, J. J. Dannenberg, V. G. Zakrzewski, S. Dapprich, A. D. Daniels, M. C. Strain, O. Farkas, D. K. Malick, A. D. Rabuck, K. Raghavachari, J. B. Foresman, J. V. Ortiz, Q. Cui, A. G. Baboul, S. Clifford, J. Cioslowski, B. B. Stefanov, G. Liu, A. Liashenko, P. Piskorz, I. Komaromi, R. L. Martin, D. J. Fox, T. Keith, M. A. Al-Laham, C. Y. Peng, A. Nanayakkara, M. Challacombe, P. M. W. Gill, B. Johnson, W. Chen, M. W. Wong, C. Gonzalez, and J. A. Pople. *Gaussian 03, Revision C.02, Gaussian, Inc., Wallingford CT*, 2004.

[10] M. Sugie, H. Takeo, and C. Matsumura. *Chem. Phys. Lett.*, 64:573, 1979.

Chapter 6

Conclusions

One of the main goals of this thesis was to investigate and describe the structure, energy, and shape of some boron-nitrogen helical structures as such molecules could be useful candidates for the synthesis of new helical boron-nitrides. Quantum-chemical computations were performed using methods based on *ab initio* and density functional theories.

The studied boron-nitrogen helices range from simple single turn type helices, *e.g.* the boron-nitrogen analogue of helicenes and phenylenes, to more complicated, laterally extended helices, such as the boron-nitrogen analogues of polymethylenyl-naphthalenes.

One particular finding of this research is the existence of a special type of isomerism resulting from alternating the boron and nitrogen atoms in the helices containing an even number of fused building units, *e.g.* the helicenes.

By taking a closer look at the investigations of these boron-nitrogen helices that were introduced in Chapter 3, 4, and 5, some conclusions can be drawn from each individual study.

Chapter 3 investigated the structure and energetics of some hydrogenated boron-nitrogen helices, the boron-nitrogen analogues of [N]helicenes, where $N = 5$, 6, 7, and 12, [N]phenylenes, where $N = 5$, 6, 7, and 13, and [6]polymethylenylnaphthalenes. Ab initio and density functional theory calculations revealed:

- The **NB** isomers are energetically more stable than their **BN** counterparts in case of the boron-nitrogen helicenes.
- The energy of helices linearly decreases with the increased number of fused structural units.
- There is a trend of electron accumulation at the peripheries of the helices, resulting in stronger bonds at the margins.

Chapter 4 presented some nonhydrogenated boron-nitrogen analogues of helicenes and their isomers comprised of fused hexagons with terminal decagons. This investigation resulted in the following conclusions:

- The initially assumed helical **BN** isomer of hexagonal units undergo a ring opening in the terminal rings.

- The ring opening stabilizes the helices, making them energetically more favorable.
- Alternating the boron and nitrogen atoms in the latter helices results in new, relatively stable isomers.
- The same trend of electron accumulation at the peripheries of the helices is observed.

Chapter 5 consists of the investigation on laterally extended boron-nitrogen helices.

- By alternating the positions of the boron and nitrogen atoms, two very similar structures are possible, the $N_xB_yH_z$ type helix and the $B_xN_yH_z$ type helix.
- The energy difference between the two types of helices is around 30 Hartrees, which is consistent with the energy difference between one boron and one nitrogen atom.
- Fusing one more hexagonal unit to these helices leads to laterally extended helical isomers with an energy difference of around 3.2-3.5 kcal/mol, depending of the level of theory used.

6.1 Future Work

Some of the future directions which could be pursued in further investigation of these boron-nitrogen helices are:

- The boron-nitrogen helices containing smaller number of units, especially the ones with six fused rings could be investigated at higher levels of theory (*e.g.* MP2)

- Inclusion of carbon atoms between the boron and nitrogen atoms in the helical structures in order to compare them with fully carbon and fully boron-nitrogen counterparts.

- Replacing the hydrogen atoms with other moieties (F, OH, CH_3) at the pheripheries could result in different electronic distribution. These effects could be the focus of further theoretical studies.

Appendix A

CUBE Keyword in Gaussian

The electron density has been evaluated using the CUBE keyword incorporated in the Gaussian software.

An example of an input file used for the calculation of electron density in case of one of the helices is shown below. Please note that instead of the Z-matrix, cartesian coordinates can be used as well.

The output file generated can be visualized with a variety of available software.

```
--start of input file
#p HF/6-31G(d) cube=(100,density,full,fine)

BN6helicene_den

0 1
 H
 H            1          B1
 H            2          B2    1          A1
 H            3          B3    2          A2     1          D1
 .            .          .     .          .      .          .
 .            .          .     .          .      .          .
 .            .          .     .          .      .          .
 N            12         B39   10         A38    9          D37
 H            40         B40   12         A39    10         D38
 N            12         B41   10         A40    9          D39

  B1          7.02641282
  B2          2.55479549
  B3          7.03880805
  .           .
  .           .
  .           .
  D37         -89.64240017
  D38         171.29409132
  D39         98.48206383

BN6helicene_den.cube

--end of input file
```

Appendix B

Atomic Units

In the description of the theory in Chapter 2 and in the results of the computational calculations in Chapter 3, Chapter 4, and Chapter 5 the units used are atomic units (a.u.). In a.u., the charge on the proton, e, the mass of the electron, m_e, and the $\hbar$ each have a numerical value of 1. Thus, the equations used are much simplified. This way the atomic unit of length will be

$$a_0 = \frac{4\pi\epsilon_0\hbar^2}{m_e e^2} \tag{B.1}$$

also called the *Bohr*. The atomic unit of energy is described as

$$E_H = \frac{\hbar^2}{m_e a_0^2}, \tag{B.2}$$

and is called the *Hartree*.

Appendix C

Visualization of Normal Modes

Throughout the thesis the flexibility and spring-like behaviour of the studied helical systems is emphasised. This is justified by the values of the vibrational frequencies.

Visualization of the spring-like motion of the lowest normal modes at some of the helices studied. Frequencies were calculated using the B3LYP/6-31G(d) optimized geometries.

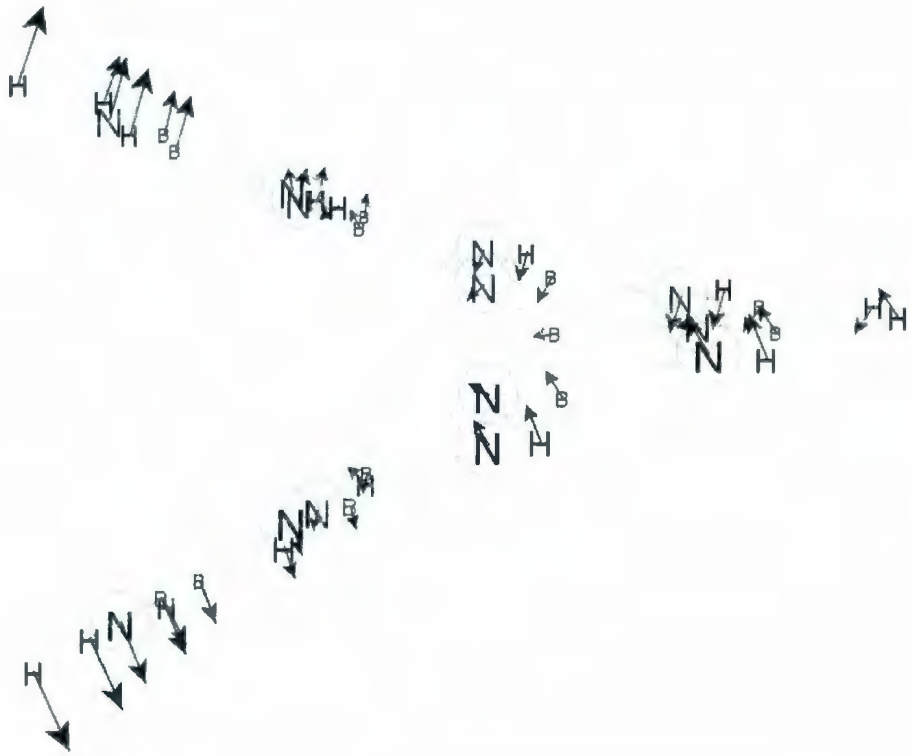

Figure C.1: Lowest normal mode of helix **3a** from Chapter 3

Figure C.2: Lowest normal mode of helix **7a** from Chapter 3

Figure C.3: Lowest normal mode of helix **6** from Chapter 4

Figure C.4: Lowest normal mode of helix **1** from Chapter 5

Figure C.5: Lowest normal mode of helix 5 from Chapter 5

Appendix D

Example of Optimization at MP2

A preliminary optimization on the boron-nitrogen helix containing six fused rings was performed at the MP2/6-31G(d) level of theory. There was no effect on the overall helical conformation.

Table D.1: The lowest wavenumbers (cm^{-1}) and ground state energies (in Hartrees) for the optimized BN[6]helicene

	MP2/6-31G(d)
Wavenumber	37.55
Total energy	-1042.4301